WSRC-STI-2007-00111

Key Words:
SASSE
Model
First Cycle
Second Cycle
Solvent Extraction
Uranium
Molybdenum
HB-Line
TBP

Retention:
Permanent

Tracking No. 10560

SASSE MODELING OF A URANIUM/MOLYBDENUM SEPARATION FLOWSHEET

J. E. Laurinat

MAY 2007

Washington Savannah River Company
Savannah River Site
Aiken, SC 29808

Prepared for the U.S. Department of Energy Under
Contract Number DE-AC09-96SR18500

SRS
savannah river site
™

DISCLAIMER

Printed in the United States of America

Prepared For
U.S. Department of Energy

REVIEWS AND APPROVALS

J. E. Laurinat, Actinide Chemical Technology Date

N. M. Askew, Technical Reviewer, Actinide Chemical Technology Date

S. D. Fink, Manager, Separations Science Programs Date

A. M. Murray, Manager, Actinide and Chemical Science Technology Date

R. A. L. Eubanks, Technical Reviewer, H-Canyon Tech Support Date

S. E. Federman, H-Canyon Engineering Manager Date

TABLE OF CONTENTS

LIST OF FIGURES

LIST OF TABLES

LIST OF ACRONYMS

1AF	Aqueous Feed to 1A Bank in First Cycle Solvent Extraction
1AS	Aqueous Scrub to 1A Bank in First Cycle Solvent Extraction
1AU	Organic Product from 1A Bank to 1B Bank in First Cycle Solvent Extraction
1AW	Aqueous Waste from 1A Bank in First Cycle Solvent Extraction
1AX	Organic Feed to 1A Bank in First Cycle Solvent Extraction
1BS	Organic Scrub to 1B Bank in First Cycle Solvent Extraction
1BP	Aqueous Product from 1B Bank in First Cycle Solvent Extraction
1BU	Organic Product from 1B Bank to 1C Bank in First Cycle Solvent Extraction
1BX	Aqueous Strip to 1B Bank in First Cycle Solvent Extraction
1CU	Aqueous Product from 1C Bank in First Cycle Solvent Extraction
1CW	Spent Organic from 1C Bank in First Cycle Solvent Extraction
1CX	Aqueous Strip to 1C Bank in First Cycle Solvent Extraction
1DF	Aqueous Feed to 1D Bank in Second Cycle Solvent Extraction
1DS	Aqueous Scrub to 1D Bank in Second Cycle Solvent Extraction
1DU	Organic Product from 1D Bank to 1E Bank in Second Cycle Solvent Extraction
1DW	Aqueous Waste from 1D Bank in Second Cycle Solvent Extraction
1DX	Organic Feed to 1D Bank in Second Cycle Solvent Extraction
1EU	Aqueous Product from 1E Bank in Second Cycle Solvent Extraction
1EW	Spent Organic From 1E Bank in Second Cycle Solvent Extraction
1EX	Aqueous Strip to 1E Bank in Second Cycle Solvent Extraction

1.0 EXECUTIVE SUMMARY

H-Canyon Engineering (HCE) is evaluating the feasibility of processing material from the Super Kukla Prompt Burst Reactor, which operated at the Nevada Test Site from 1964 to 1978. This material is comprised of 90 wt % uranium (U) (at approximately 20% ^{235}U enrichment) alloyed with 10 wt % molybdenum (Mo).[1] The objective is to dissolve the material in nitric acid (HNO_3) in the H-Canyon dissolvers and then to process the dissolved material through H-Canyon First and Second Cycle solvent extraction. The U product from Second Cycle will be sent to the highly enriched uranium (HEU) blend down program. In the blend down program, enriched U from the 1EU product stream will be blended with natural U at a ratio of 1 part enriched U per 3.5 parts natural U to meet a reactor fuel specification of 4.95% ^{235}U before being shipped for use by the Tennessee Valley Authority (TVA) in its nuclear plants.[2] The TVA specification calls for <200 μg Mo/g U (200 ppm). Since natural U has about 10 μg Mo/g U, the required purity of the 1EU product prior to blending is about 800 μg Mo/g U, allowing for uncertainties.

HCE requested that the Savannah River National Laboratory (SRNL) define a flowsheet for the safe and efficient processing of the U-10Mo material.[1] This report presents a computational model of the solvent extraction portion of the proposed flowsheet. The two main objectives of the computational model are to demonstrate that the Mo impurity requirement can be met and to show that the solvent feed rates in the proposed flowsheet, in particular to 1A and 1D Banks, are adequate to prevent refluxing of U and thereby ensure nuclear criticality safety.

SASSE (Spreadsheet Algorithm for Stagewise Solvent Extraction), a Microsoft Excel spreadsheet that supports Argonne National Laboratory's proprietary AMUSE (Argonne Model for Universal Solvent Extraction) code,[3] was selected to model the U/Mo separation flowsheet. SASSE spreadsheet models of H-Canyon First and Second Cycle solvent extraction show that a standard unirradiated fuel flowsheet is capable of separating U from Mo in dissolved solutions of a U/Mo alloy. The standard unirradiated fuel flowsheet is used, except for increases in solvent feed rates to prevent U refluxing and thereby ensure nuclear criticality safety and substitution of higher HNO_3 concentrations for aluminum nitrate ($Al(NO_3)_3$) in the feed to 1A Bank. (Unlike Savanah River Site (SRS) fuels, the U/Mo material contains no aluminum (Al). As a result, higher HNO_3 concentrations are required in the 1AF to provide the necessary salting.)

The TVA limit for the final blended product is 200 μg Mo/g U, which translates to approximately 800 μg Mo/g U for the Second Cycle product solution. SASSE calculations give a Mo impurity level of 4 μg Mo/g U in the Second Cycle product solution, conservatively based on Mo organic-to-aqueous distributions measured during minibank testing for previous processing of Piqua reactor fuel. The calculated impurity level is slightly more than two orders of magnitude lower than the required level. The Piqua feed solution contained a significant concentration of $Al(NO_3)_3$, which is not present in the feed solution for the proposed flowsheet. Measured distribution data indicate that, without $Al(NO_3)_3$ or other salting agents present, Mo extracts into the organic phase to a much lesser extent, so that the overall U/Mo separation is better and the Mo impurities in the Second Cycle product drop to negligible concentrations.

The 1DF U concentration of 20 g/L specified by the proposed flowsheet requires an increased 1DX organic feed rate to satisfy H-Canyon Double Contingency Analysis (DCA) guidelines for

the prevention of U refluxing.[4] The ranges for the 1AX, 1BS, and 1DX organic flow rates in the proposed flowsheet are set so that the limiting ratios of organic/aqueous flow rates exactly meet the minimum values specified by the DCA.[4]

2.0 INTRODUCTION

HCE is evaluating the feasibility of processing material from the Super Kukla Prompt Burst Reactor, which contains 90 wt % U (20% ^{235}U enrichment) alloyed with 10 wt % Mo.[1] The objective is to dissolve the material in HNO_3 in the H-Canyon dissolvers and then to process the dissolved material through H-Canyon First and Second Cycle solvent extraction processes. The U product from Second Cycle will be sent to the HEU blend down program. In the blend down program, enriched U from the 1EU product stream will be blended with natural U at a ratio of 1 part enriched U per 3.5 parts natural U to meet a reactor fuel specification of 4.95% ^{235}U before being shipped for use by the TVA in its nuclear plants.[2] The TVA specification calls for <200 μg Mo/g U (200 ppm). Since natural U has about 10 μg Mo/g U, the required purity of the 1EU product prior to blending is about 800 μg Mo/g U, allowing for uncertainties.

HCE requested that SRNL define a flowsheet for the safe and efficient processing of the U-10Mo material.[1] This report presents a computational model of the solvent extraction portion of the proposed flowsheet. The two main objectives of the computational model are to demonstrate that the Mo impurity requirement can be met and to show that the solvent feed rates in the proposed flowsheet, in particular to 1A and 1D Banks, are adequate to prevent refluxing of U and thereby ensure nuclear criticality safety.

3.0 SASSE MODEL

SASSE was selected to model the U/Mo separation flowsheet. SASSE is a standalone Microsoft Excel macro developed by Argonne National Laboratory to support their proprietary AMUSE solvent extraction code.[3] SASSE was substituted for the SEPHIS (Solvent Extraction Process Having Interacting Solvents) computer code that historically has been used to model solvent extraction flowsheets at SRS.[5] The need to model the extraction behavior of Mo necessitated the switch from SEPHIS to SASSE. SEPHIS is restricted to modeling of the standard Purex process, since it contains distribution models for only HNO_3, U, plutonium(Pu)(III), and Pu(IV). Any attempt to add a model for the separation of Mo would require extensive code modifications, followed by a significant effort to place the modified version of SEPHIS back under configuration control. This work could not be completed in a timely manner to allow the modeling of the proposed flowsheet. SASSE, by contrast, allows user inputs of arbitrary chemical species such as Mo, including expressions for distribution coefficients. Thus, SASSE is ideally suited for modeling nonstandard flowsheets, such as those recently used to separate neptunium (Np) from H-Canyon tank solutions.[6,7]

Input items for the SASSE spreadsheet include the number of stages, the feed and product stream locations, flow rates and compositions, organic and aqueous volumes, separation efficiencies, entrainments for each stage, and distribution coefficients for each stage. The distribution

coefficients may be entered as functions of the aqueous concentrations in the stage. The SASSE models are limited to one bank and are normally set up for an organic feed to the first stage, an aqueous feed to an intermediate stage, and an aqueous scrub to the last stage.

Separate SASSE spreadsheet models were prepared for the proposed U/Mo separation flowsheet and for the minibank tests on the Hallam and Piqua reactor fuels. SRS received that fuel from the Hallam, Nebraska, and the Piqua, Ohio, reactors, both of which were decommissioned from 1967 to 1969. Minibank tests were performed prior to the processing of the Piqua fuel, a 96 wt % U, 4 wt % Mo alloy, in 1973.[8] Similar minibank tests were conducted before processing the Hallam fuel, a 90 wt % U, 10 wt % Mo alloy, in 1979.[9] Both tests included simulations of A and B Banks from First Cycle Solvent Extraction. The objective of the modeling of the Hallam and Piqua tests was either to confirm that Mo distribution coefficient correlations based on literature data are applicable or to develop new Mo distribution coefficient correlations by fitting the results of SASSE calculations to the measured Mo decontamination factors (DFs) for the product solutions.

Figure 3-1 and 3-2 depict the SASSE models of the H Canyon 1A, 1B, 1C, 1D, and 1E Banks for the proposed solvent extraction separation of U and Mo. Separate SASSE calculations are used to model each bank. The models for each bank are "manually" connected by specifying the organic product from one bank as the feed to the following bank. Specifically, the organic product from 1A Bank (1AU) is the intermediate feed to 1B Bank, the organic product from 1B Bank (1BU) is the feed to 1C Bank, the aqueous product from 1C Bank (1CU), after evaporation and HNO_3 addition, is the feed to 1D Bank (1DF), and the organic product from 1D Bank (1DU) is the feed to 1E Bank.

Table 3-1 lists the flow rates, temperatures, and compositions used by SASSE to model the proposed flowsheet. The flow rates are based largely on recent First Cycle operating experience with unirradiated Mark 22 assemblies and Idaho National Laboratory (INL) blended materials.[10] There is only one significant difference between the unirradiated fuel flowsheet and the proposed U/Mo separation flowsheet. The difference is the replacement of $Al(NO_3)_3$ with higher HNO_3 concentrations in the 1AF feed for the U/Mo flowsheet.

The effect of the increase in the HNO_3 concentration in the proposed flowsheet on the Mo solubility is examined in Section 5.

HNO_3 concentrations are specified at 0.01 M in 1AX, 1BS, 1CX, 1DX, and 1EX. The model also includes Mo(VI), U(VI), Pu(III), and Pu(IV). Pu is modeled to account for the distribution of possible trace concentrations of Pu from process contamination; the 1AF feed solutions does not contain any Pu. Feed concentrations for HNO_3, Mo(VI), and U(VI) are expressed in molar units. The feed concentration for Pu(IV) is set at a nominal concentration equal to a fraction of the concentration in the aqueous feed, 1AF, to allow a direct calculation of DFs.

The mixer-settler stages in 1A and 1B Banks have the same dimensions, so they should hold the same aqueous and organic volumes. The volumes in 1C Bank are larger. The aqueous and organic volumes contained in each stage depend to a small extent on the relative flow rates of the

organic and aqueous phases. Table 3-2 lists the formulas used to compute the total organic and aqueous volumes contained in each stage.[11,12]

Equilibrium stage efficiencies and entrainment ratios were estimated in previous modeling studies for Np separation.[6,7] The equilibrium stage efficiencies for A and B Banks were calculated by matching measured and calculated thorium DFs for the 2A Bank, and the aqueous entrainment in the organic phase was calculated by matching measured and calculated neptunium losses for the 2B Bank. The aqueous entrainment in the organic phase has been determined for both A and B Banks using historical operating data. For the 1A Bank, two separate calculations gave aqueous-in-organic entrainments of 0.65 and 0.68 vol %.[13,14] The SASSE models for both the validation case (using the Hallam and Piqua fuels) and the proposed flowsheet use the average of these two values, which is 0.665 vol %. Measured aqueous entrainments in the organic phase for B Bank range from 1.24 vol % to 2.33 vol % at normal flow rates,[15] and from 4.0 vol % to 9.3 vol % at high flow rates.[16] These studies did not report any measurable organic entrainment in the aqueous phase. In view of the wide range of reported B Bank entrainments, the B Bank aqueous-in-organic entrainment was fitted using the Np(VI) flowsheet validation calculations. An entrainment ratio of 1.75 vol % was calculated.[6] Because there were no reports of organic-in-aqueous entrainment, the organic in aqueous entrainment for both A and B Banks was set at zero. The entrainments for C, D, and E Banks were set at the same values used for B Bank.

Input conditions for the SASSE models of the minibank tests for the Hallam and Piqua fuels are listed in Table 3-3. It may be noted that the input HNO_3 concentration (i.e., the 1AF HNO_3 concentration) includes three NO_3^- equivalents for the molar concentration of ferric nitrate ($Fe(NO_3)_3$) in the Hallam feed and $Al(NO_3)_3$ in the Piqua feed. The rationale is that both the iron (Fe) and the Al remain as ionic species in the aqueous phase in A Bank and thus contribute to the overall NO_3^- aqueous concentration. No such adjustment is made for the U in the feed, which mostly extracts into the organic phase. Table 3-3 also lists the measured DFs for A and B Banks. These DFs are used to fit average distribution coefficients for A and B Banks, as explained in Section 4.

Mixing stage aqueous and organic volumes, the aqueous in organic entrainment ratio, and the equilibrium stage efficiency for the minibanks were provided by M. L. Crowder, who has recent experience operating the minibanks.[17] The estimated aqueous volume in each stage is 60 mL, and the estimated organic volume is 90 mL. The recommended value for the aqueous entrainment in the organic phase is 1 vol %, and the recommended stage efficiency is 70%. These values apply to both A and B Banks. The minibanks are set up identical to the First Cycle A and B Banks in that each minibank contains 16 equilibrium stages, with the feed entering on Stage #8.

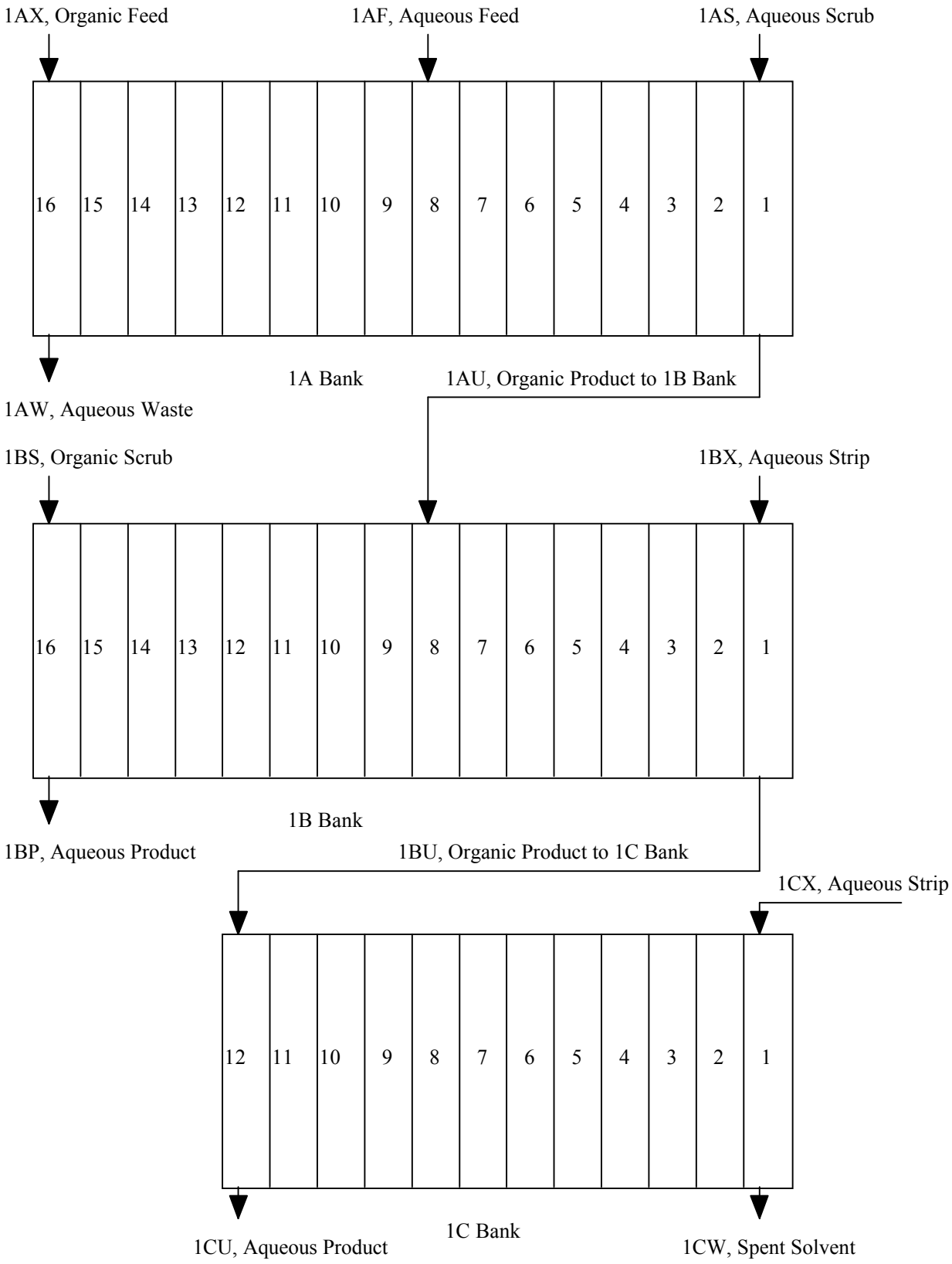

Figure 3-1. First Cycle Flowsheet

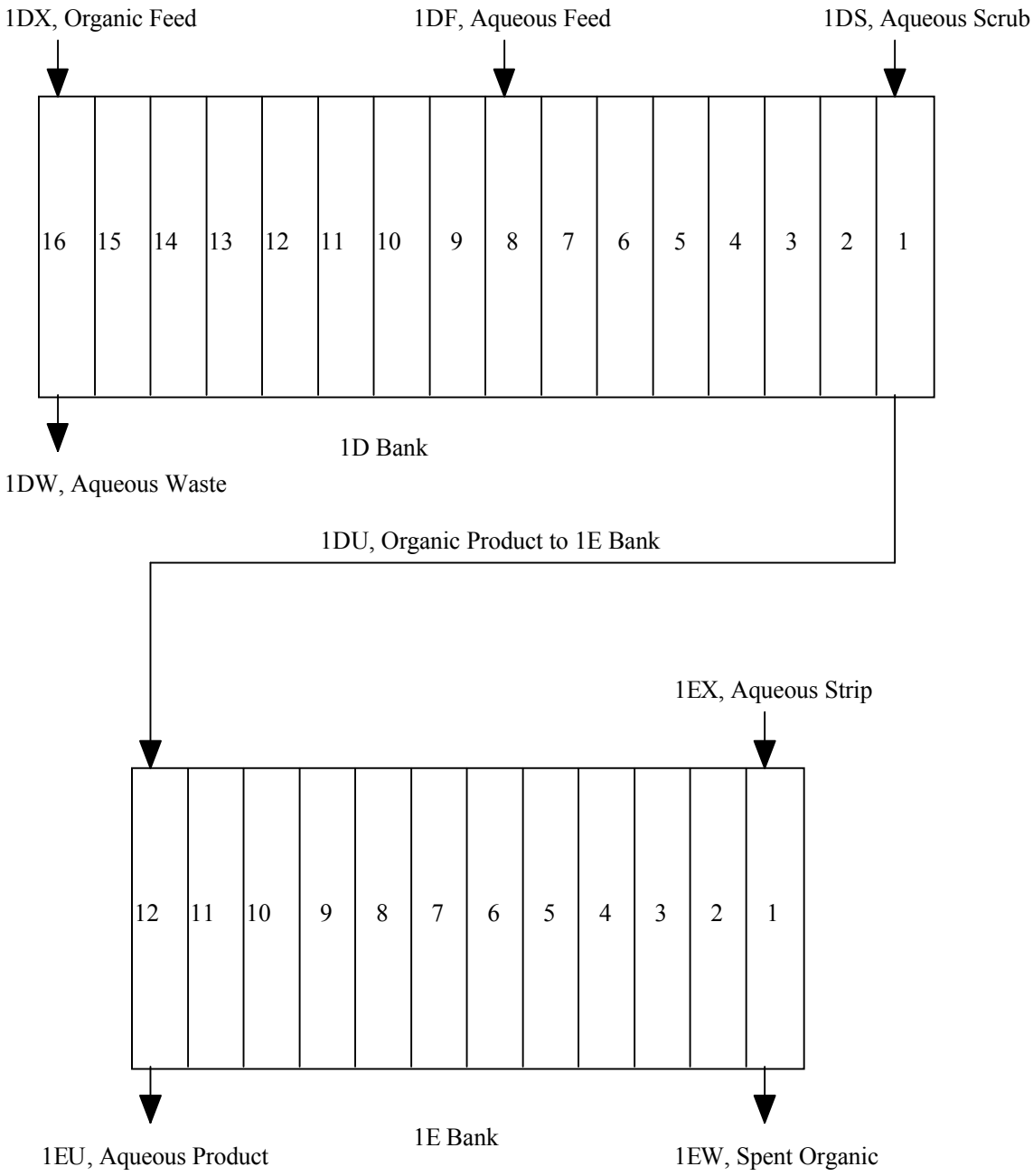

Figure 3-2. Second Cycle Flowsheet

Table 3-1. Flow Rates, Temperatures, and Compositions for Proposed U/Mo Separation Flowsheet

Parameter	Units	Minimum	Nominal	Maximum
1AF flow	lbm/min	14.2	15.6	17.5
	L/min	5.65	6.21	6.95
1AS flow	lbm/min	3.6	4.0	4.5
	L/min	1.48	1.63	1.82
1AX flow[a]	lbm/min	19.8	21.0	22.3
	L/min	11.23	11.91	12.62
1BS flow[a]	lbm/min	32.7	35.0	37.5
	L/min	18.55	19.84	21.23
1BX flow	lbm/min	13.2	14.0	14.84
	L/min	5.69	6.03	6.39
1CX flow[c]	lbm/min	20.6	22.0	23.5
	L/min	9.32	9.97	10.67
1AS temperature	° C	34	38	43
1AX temperature	° C	35	40	43
1BS temperature	° C	35	39	43
1BX temperature	° C	32	36	43
1CX temperature	° C	50	60	65
1AF [U][b]	g/L		15	
	M		0.0632	
1AS [HNO_3]	wt %	20	22	25
	M	3.50	3.87	4.42
1BX [FS][d]	M	0.015	0.02	0.025
1BX [HNO_3]	M	1.48	1.53	1.58
1DF flow	lbm/min	16.5	18.5	20.5
	L/min	6.62	7.38	8.13
1DS flow	lbm/min	8.15	9.51	9.74
	L/min	3.6	4.2	4.3
1DX flow[a]	lbm/min	58.0	59.08	61.7
	L/min	32.93	33.5	35.0
1EX flow	lbm/min	7.1	12.5	19.0
	L/min	4.13	7.27	11.05
1DF temperature	° C	5	38	44
1DS temperature	° C	20	35	44
1DX temperature	° C	20	35	44
1EX temperature	° C	50	60	65
1DF [HNO_3]	M	3.9	4.3	5.8
1DF [U][b]	g/L		20	
	M		0.0847	
1DS [HNO_3]	wt %	5.2	5.5	6.0
	M	0.85	0.90	0.98
1DS [FS][d]	M	0.045	0.047	0.05

[a] The 1AX, 1BS,and 1DX flow rates are set to comply with the DCA limits to prevent the possibility of U reflux in 1A, 1B, and 1D Banks.[3]

[b] The nominal U concentrations in 1AF and 1DF represent the First and Second Cycle feed concentration for the proposed flowsheet. The Mo concentration is scaled so that the ratio of Mo to U is the same in 1DF as in 1CU. (The U/Mo ratio will not change, provided that Mo does not precipitate during the Second Cycle feed adjustment.)

[c] The 1CX stream may be operated at flow rates higher than listed without causing any adverse impact to the approved flowsheet. The 1CX stream may be operated at flow rates lower than listed without causing any adverse impact to the proposed flowsheet, provided that the H-Canyon DCA requirements[4] are met.

[d] FS is added to 1BX and 1DS to reduce any Pu that might be present to Pu(III), so that the Pu will strip into 1BP and 1DW.

Table 3-2. Aqueous and Organic Volumes in A, B, C, D, and E Banks

	Aqueous	Organic
A, B, and D Banks		
Mixer Volume (L/stage)	$2.36 + 9.439\frac{Q_{aq}}{Q_{aq}+Q_{or}}$	$9.439\frac{Q_{or}}{Q_{aq}+Q_{or}}$
Settler Volume (L/stage)	21.1	42.1
Total Volume (L/stage)	$23.46 + 9.439\frac{Q_{aq}}{Q_{aq}+Q_{or}}$	$42.1 + 9.439\frac{Q_{or}}{Q_{aq}+Q_{or}}$
C and E Banks		
Mixer Volume (L/stage)	$6.637 + 25.22\frac{Q_{aq}}{Q_{aq}+Q_{or}}$	$25.22\frac{Q_{or}}{Q_{aq}+Q_{or}}$
Settler Volume (L/stage)	84.93	169.83
Total Volume (L/stage)	$91.567 + 25.22\frac{Q_{aq}}{Q_{aq}+Q_{or}}$	$169.83 + 25.22\frac{Q_{or}}{Q_{aq}+Q_{or}}$

Note: Q_{aq} and Q_{or} represent the aqueous and organic phase flow rates in L/min.

Table 3-3. Simulation Conditions for Hallam and Piqua Tests

Parameter	Units	Hallam Tests		Piqua Tests			
		#1	#2	#1	#2	#3	#4
1AS/1AF	vol flow ratio	0.575	0.575	0.3	0.345	0.345	0.345
1AX/1AF	vol flow ratio	5	5	3	3	3	3
1BS/1AF	vol flow ratio	3	3	1.5	1	1	1.5
1BX/1AF	vol flow ratio	1	1	0.5	0.5	0.5	0.5
1AF [HNO_3]	M	3.34[a]	3.75[a]	4.44[b]	3.8[b]	4.31[c]	5.58[d]
1AS [HNO_3]	M	4	4	4.12	4.32	3.76	4.16
1BX [HNO_3]	M	2	2	1.56	2.16	1.87	1.97
1AF [U]	g/L	76.0	80.3	27.0	24.8	23.6	26.4
	M	0.319	0.337	0.113	0.104	0.099	0.111
Mo DF, 1BP	1AF/1BP	500	1700	2500	4000	2900	1400
Mo DF, 1BU	1AF/1BU	25	65	2.4	5.4	20	18

Notes:
[a] Includes 2.16 M HNO_3 from 0.72 M Fe.
[b] Includes 0.36 M HNO_3 from 0.12 M Al.
[c] Includes 0.33 M HNO_3 from 0.11 M Al.
[d] Includes 1.44 M HNO_3 from 0.48 M Al.

4.0 DISTRIBUTION COEFFICIENT CORRELATIONS

The SASSE model for the proposed flowsheet includes distribution coefficients for HNO_3, U(VI), Mo(VI), Pu(III), and Pu(IV). The Pu distribution coefficients are included to model the distribution of any Pu that might be introduced by contamination. The distributions coefficients for HNO_3, U(VI), Mo(VI), and Pu(III) are based on measured data from the Savannah River Site (SRS), and the distribution coefficients for Pu(IV) are based on data from SRS and other sources. The distribution coefficients are correlated as functions of the HNO_3 concentration in the aqueous phase.

Distribution coefficients for HNO_3 and for U(VI) in 7.5 vol % tributyl phosphate (TBP) have been measured.[18,19] Previously, these measured distribution coefficients were correlated in terms of the molar concentration of HNO_3 in the aqueous phase, $[HNO_3]$, and the U concentration in the organic phase in g/L, $[U(VI)]_{or}$, by the following expressions:[20]

$$\begin{aligned} D_{\%_a,HNO_3} &= 0.0571 - 0.0236[HNO_3] + 0.00607[HNO_3]^2 \\ &- 0.00203[U(VI)]_{or} + 0.0000841[U(VI)]_{or}^2 - 0.00000182[U(VI)]_{or}^3 \end{aligned} \quad (1)$$

and

$$D_{\%_a,U(VI)} = \exp\left(\begin{aligned} &-0.304 + 1.53\ln([HNO_3]) - 0.291(\ln([HNO_3]))^2 \\ &-0.226\ln([U(VI)]_{or}) + 0.326(\ln([U(VI)]_{or}))^2 - 0.129(\ln([U(VI)]_{or}))^3 \end{aligned}\right) \quad (2)$$

where $D_{\%_a,HNO_3}$ is the organic-to-aqueous distribution coefficient for HNO_3 and $D_{\%_a,U(VI)}$ is the distribution coefficient for U.

Use of these correlations in SASSE models gave spurious oscillations in the computed distribution profiles across the banks of equilibrium stages. These oscillations probably resulted from either the use of polynomial expressions or the use of both aqueous and organic phase concentration terms. To avoid this oscillatory behavior, asymptotic equations for HNO_3 and U distribution coefficients were fit to the data from Reference 14 for the proposed flowsheet model conditions (45 °C and 7.5 vol % TBP). The asymptotic equations are functions of the aqueous HNO_3 concentration, or the minimum of the aqueous HNO_3 concentration and half the aqueous U concentration. The asymptotic equations are expressed as the minimum of a power law fit to the data at low HNO_3 and U concentrations and an asymptotic upper bound to the data at higher HNO_3 and U concentrations. The upper bounds, in turn, are correlated in terms of an absolute upper bound at low HNO_3 concentration and a power law fit to the upper bound of the data at higher HNO_3 concentrations.

The overall expression for the HNO_3 distribution coefficient, $D_{\%_a,HNO_3}$, takes the form

$$D_{\%_a,HNO_3} = \min\left(D_{\%_a,HNO_3,asy}, D_{\%_a,HNO_3,la}\right) \quad (3)$$

where $D_{o/a,HNO_3,asy}$ is the upper asymptote to the HNO_3 distribution coefficient at high HNO_3 and U concentrations and $D_{o/a,HNO_3,la}$ represents the low HNO_3 correlation of the distribution coefficient.

The HNO_3 distribution coefficient at low HNO_3 concentrations is correlated in terms of the total nitrate concentration, which is calculated as the sum of the HNO_3 concentration and twice the U concentration; this assumes that the U is present in the aqueous solutions as uranyl nitrate ($UO_2(NO_3)_2$). A power law fit gives

$$D_{o/a,HNO_3,la} = 0.0281[NO_3^-]^{0.6607} \quad (4)$$

where $[NO_3^-] = [HNO_3] + 2[UO_2(NO_3)_2]$ (5)

(Note: All concentrations in equation 4 and following equations are in molar units. The NO_3^- concentration refers to the total NO_3^- concentration, whereas the HNO_3 concentration refers to the concentration of NO_3^- not associated with a metal cation.)

The regression fit for this correlation is shown by Figure 8-1 in the Appendix.

The expression for upper asymptote to the HNO_3 distribution coefficient takes the form

$$D_{o/a,HNO_3,asy} = \left(\frac{1}{\left(\frac{1}{0.05}\right)^3} + \frac{1}{\left(0.0098\left(\min\left([HNO_3],0.5[U]\right)\right)^{-0.3828}\right)^3} \right)^{1/3} \quad (6)$$

Figure 8-2 illustrates the regression fit for the high HNO_3 range portion of the asymptote. It may be noted that the regression is in terms of the minimum of the HNO_3 concentration and half the U concentration. It was found that this combination collapsed the data at high HNO_3 concentrations to a single-valued maximum. Figure 8-3 compares the upper asymptote given by equation 6 with all of the HNO_3 distribution data. The comparison shows that the distribution data fall on or below the asymptotic curve.

The most straightforward way to illustrate the regression fit of the HNO_3 distribution data given by equations 3 through 6 is to plot predicted values for the distribution coefficients against the measured values, as shown by Figure 8-4. This plot demonstrates that the regression provides an adequate fit; much of the scatter exhibited at lower values of the distribution coefficient may result from round-off errors in the organic phase concentration data.

The overall equation for the U distribution coefficient, $D_{o/a,U(VI)}$, takes the form

$$D_{\%a,U(VI)} = \min\left(D_{\%a,U(VI),asy}, D_{\%a,U(VI),la}\right) \quad (7)$$

where $D_{\%a,U(VI),asy}$ is the upper asymptote to the U distribution coefficient at high HNO_3 and U concentrations and $D_{\%a,U(VI),la}$ is the low HNO_3 correlation of the distribution coefficient.

The low HNO_3 correlation is expressed as a power law fit against the total nitrate concentration, divided by a U "salting factor", $s_{U(VI)}$:

$$D_{\%a,U(VI),la} = \frac{0.5956[NO_3^-]^{1.4833}}{s_{U(VI)}} \quad (8)$$

The power law term in the numerator of equation 8 was calculated by fitting data at low U and HNO_3 concentrations, as shown by Figure 8-5.

The so-called "salting factor" in the denominator of equation 8 accounts for an observed reduction in the U distribution coefficient at intermediate U concentrations below the concentration where the distribution coefficient approaches its upper asymptote. The "salting factor" is correlated as the product of an exponential function of the HNO_3 concentration and a factor $f_{U(VI)}$, which is the fraction of nitrate that complexes with U, assuming that U(VI) combines to form $UO_2(NO_3)_2$. The "salting factor" is limited to values between one and two. The expression for the "salting factor" is

$$s_{U(VI)} = \min\left(2, \exp\left(0.1784\exp\left(1.7082[HNO_3]\right)f_{U(VI)}\right)\right) \text{ if } [HNO_3] < 1.5 \quad (9)$$

and

$$s_{U(VI)} = 1 \text{ if } [HNO_3] \geq 1.5 \quad (10)$$

where

$$f_{U(VI)} = \frac{2[UO_2(NO_3)_2]}{[HNO_3] + 2[UO_2(NO_3)_2]} \quad (11)$$

The exponential terms in equation 9 were determined by plotting the ratio of the distribution coefficient predicted by the numerator of equation 8 as a function of $f_{U(VI)}$ at several HNO_3 concentrations, as shown in Figure 8-6. The slopes of the regression fits at each HNO_3 concentration from Figure 8-6 were then plotted against the HNO_3 concentration, and a regression was performed to calculate the factors which appear in equation 9. This regression is depicted by Figure 8-7.

The upper asymptote to the U distribution coefficient is correlated as a function of the U concentration. The asymptotic correlation takes the form

$$D_{\%_a,U(VI),asy} = \left(\frac{1}{(0.25)^{1.5}} + \frac{1}{\left(0.1238[U]^{-0.8272}\right)^{1.5}} \right)^{1/1.5} \quad (12)$$

Figure 8-8 shows the regression fit for the high U concentration portion of this asymptotic expression. Figure 8-9 compares the asymptotic expression in equation 12 with all of the U distribution data. This comparison demonstrates that the upper asymptote bounds all of the data. Figure 8-10 illustrates the fit of the regression given by equations 7 through 12; the comparison of predicted and measured values shows that the regression of the data is acceptable over a wide range of distribution coefficients.

The distribution coefficient for Pu(III) was correlated as part of the SASSE modeling of a reducing Np(IV) flowsheet.[7] The Pu(III) distribution coefficient is scaled linearly to measured distribution coefficients for HNO_3 solutions in contact with 19 vol % TBP and 36 vol % TBP in kerosene at 19 to 23 °C.[21,22,23] The 7.5 vol % TBP correlation used to model the proposed flowsheet is scaled to the 19 vol % TBP data, and the 30 vol % TBP correlation used for the validation calculations is scaled to the 36 vol % TBP data. Such scaling should yield conservatively high values for estimated distribution coefficients, since the measured 36 vol % TBP coefficients are more that twice the measured 19 vol % TBP coefficients. There was no attempt to correct the Pu(III) distribution coefficient for temperature effects.

The estimated Pu(III) distribution coefficients are based on power-law regressions of measured distribution data for solutions below about 2 M HNO_3, which are illustrated in Figure 8-11, and maximum measured distribution ratios at approximately 2 M HNO_3. The resulting asymptotic expressions for the Pu(III) distribution coefficients for HNO_3 solutions in contact with 7.5 vol % TBP for the proposed flowsheet is:

$$D_{\%_a,Pu(III)} = \min\left(0.0163, 0.00209[NO_3^-]^{0.9865}\right) \quad (13)$$

The Pu(IV) distribution coefficient is based primarily on data for HNO_3 solutions in contact with 19 to 30 vol % TBP,[20] from SRS and elsewhere.[22,23,24,25] The distribution coefficients at higher TBP concentrations are adjusted downward to equivalent values for 7.5 vol % TBP by multiplying by the ratio of 7.5 vol % to the respective vol % TBP for the data, taken to the 1.4 power. The exponent is based on a correlation of distribution coefficients at 7 M HNO_3 and various TBP concentrations,[25] shown in Figure 8-12. The regression of the adjusted distribution coefficients is depicted by Figure 8-13. The expression for the Pu(IV) distribution coefficient combines the regression correlation shown in Figure 8-13 in an asymptotic equation with the estimated maximum measured coefficient for 6.5 M HNO_3, which is 6.88. The specification of a maximum value for the distribution coefficient is consistent with the form of the distribution coefficient equations for Pu(III) and other actinide species, which exhibit maximum distribution coefficients at high HNO_3 concentrations. The final form of the expression for the Pu(IV) distribution coefficient is

$$D_{o/a,Pu(IV)} = \min\left(6.88, 0.37[NO_3^-]^{1.5619}\right) \quad (14)$$

Distribution coefficients for Mo(VI) have been measured by Vorob'ev et al.,[26] Fujii et al.,[27] and Visser and Pierce.[28] These distribution coefficients are compared with distribution coefficients fitted to the DFs reported for the small scale Hallam and Piqua fuel tests, listed in Table 3-3. The Hallam and Piqua tests were conducted with slightly more concentrated solutions than were used in the Vorob'ev et al. and Fujii et al. studies; the Visser and Pierce tests used a simulant of the 1AF feed solution in contact with 7.5 vol % TBP and thus approximately simulated conditions in the 1A Bank in the proposed flowsheet. (The aqueous Mo concentrations were 0.01 to 0.0176 M for the Hallam tests and 0.09 M for the Piqua tests versus 0.0001 to 0.01 M for Vorob'ev et al., 0.0017 M for Fujii et al., and 0.019 M for Visser and Pierce. None of these concentrations exceed the Mo solubility limits. The highest Mo concentration, for the Piqua tests, was achieved with the addition of Fe, which complexes with Mo and increases its solubility.[29,30])

Three separate SASSE models were constructed using Mo(VI) distribution coefficients based on the Hallam, the Piqua, and the Visser and Pierce data. Distribution coefficients were fitted to the Hallam and Piqua test results by running SASSE to match computed DFs to the measured DFs. Separate distribution coefficients were calculated for A and B Bank test simulations. For each bank, the Mo(VI) distribution coefficient in the SASSE model was kept constant across all the stages. The HNO_3 concentration corresponding to the distribution coefficient was estimated by averaging the HNO_3 concentrations over the stages of each bank. The distribution coefficient was varied to obtain a match between the computed and measured DF for each bank by a trial and error process. Table 4-1 lists the results of the SASSE computations.

Table 4-1. SASSE Calculations of Mo(VI) Distribution Coefficients for Hallam and Piqua Tests

Test	Bank	Average [HNO_3], M	$D_{o/a}$, Mo(VI)
Hallam Test 1	A	3.63	0.085
	B	2.45	0.43
Hallam Test 2	A	3.82	0.064
	B	2.45	0.465
Piqua Test 1	A	4.25	0.239
	B	2.32	1.08
Piqua Test 2	A	4.00	0.166
	B	2.69	1.39
Piqua Test 3	A	4.00	0.102
	B	2.39	0.95
Piqua Test 4	A	4.85	0.106
	B	2.57	0.59

Figure 8-14 compares the fitted distribution coefficients for the Hallam and Piqua tests with the measured values. As Figure 8-14 shows, the Hallam and Piqua distribution coefficients are from one to three orders of magnitude higher than the measured distribution coefficients at the same HNO_3 concentration. The differences between the Hallam and Piqua distribution coefficients and the measured values can be attributed to the salting effects of the Fe and Al present in the Hallam and Piqua feed solutions, respectively. The presence of these metal ions increases both the solubility and the extractability of Mo by forming soluble and extractable ferri- and alumino-polymolybdates in acid solutions.

One may note that the Mo(VI) distribution coefficients for the Hallam and Piqua tests and for the Fujii et al. tests with U in solution increase as the HNO_3 concentration decreases. This increase may be attributed to the fact that Mo forms molybdic acid anionic species that would extract with U much as NO_3^- does.[8] If Mo extracts as an acid, then it likely would extract with U to a greater extent at lower total HNO_3 concentrations due to the increased availability to complex with U compared with the NO_3^- that remains.

The fitted Mo(VI) distribution coefficients for the Piqua tests are two to three times higher than those for the Hallam tests, both of which used processing conditions similar to those of the proposed flowsheet. For this reason, separate correlations were developed for the Hallam and Piqua tests. The regressions of the Hallam and Piqua distribution coefficients are depicted in Figure 8-15.

The correlation equation for the Hallam distribution coefficients takes the form

$$D_{\%a,Mo(VI)} = \min\left(10, 21.476[HNO_3]^{-4.3208}\right) \quad (15)$$

The Piqua distribution coefficients are correlated by

$$D_{\%a,Mo(VI)} = \min\left(10, 19.194[HNO_3]^{-3.3416}\right) \quad (16)$$

Equations 15 and 16 both limit the distribution coefficient to a maximum value of 10 at low HNO_3 concentrations. This limit was added to avoid numerical difficulties at the very low HNO_3 concentrations encountered in 1C and 1E Banks. A distribution coefficient of 10 is sufficient to give virtually quantitative extraction of all Mo into the organic phase at low HNO_3 concentrations.

The distribution coefficient for the Visser and Pierce tests is correlated by combining the worst case (highest) distribution coefficient measured by Visser and Pierce with the results measured by Fujii et al. for solutions containing 0.25 M U. As Figure 8-14 illustrates, the distribution coefficients measured by Fujii et al. with U present are lower than those measured by Visser and Pierce at the same HNO_3 concentration, but increase as the HNO_3 concentration decreases, presumably due to salting by the U. To account for this increase in the measured distribution coefficient, the Visser and Pierce tests are correlated using the following asymptotic combination of their worst case distribution coefficient, 0.003, with the regressed correlation of the Fujii et al. data for solutions containing U, shown by Figure 8-16. The resulting expression takes the form

$$D_{\%a,Mo(VI)} = \max\left(0.0030, \min\left(10, 0.0008205[HNO_3]^{-1.3155}\right)\right) \quad (17)$$

It may be noted that the distribution coefficient is restricted to values less than or equal to 10, as was done for the Hallam and Piqua correlations.

Distribution coefficients for the SASSE flowsheet model are evaluated at 45 °C. Actual temperatures may differ slightly from the temperature used for the SASSE flowsheet model. The nominal operating temperatures for 1A, 1B, and 1D Banks range between 35 °C and 40 °C (see Table 3-1). The distribution coefficients for U(VI) and Pu(IV) decrease as the temperature increases.[18,22] One may assume that the decrease in the distribution coefficients results from a general tendency of metal ions to associate with NO_3^- ions to form extractable complexes to a lesser extent as temperatures increase; if this assumption holds, then the distribution coefficients for Mo(VI) and Pu(III) also should decrease as the temperature increases. It follows that, at the lower temperatures for 1A, 1B, and 1D Banks, the modeled solution components would extract into the organic phase somewhat better than predicted by the SASSE model. The nominal operating temperature for 1C and 1E Banks is 60 °C. At this elevated temperature, the modeled solution components should strip into the aqueous phase better than predicted by SASSE.

5.0 PREDICTIONS FOR PROPOSED FLOWSHEET

SASSE models of the proposed U/Mo separation flowsheet were prepared using the nominal flow rates and compositions from Table 3-1 and the distribution coefficient correlations listed in Section 4. Because the correlations of the Hallam and Piqua data gave significantly different values for Mo distribution coefficients, separate SASSE models were built based on the Hallam distribution coefficient correlation (equation 15) and the Piqua distribution coefficient correlation (equation 16). As a result, there are two separate SASSE models.

The distribution coefficient correlations, except for the correlations for Pu(III) and Pu(IV), which are evaluated at approximately 25 °C, are for solutions at 45 °C, so the effective temperature for the model is 45 °C in all banks. No adjustment was made to account for differences between the model temperature of 45 °C and the nominal temperatures listed in Tables 3-1 and 3-2. Since Mo compounds show an inverse correlation of solubility with temperature,[29] this simplification should prove to be conservative for 1A Bank, which has the highest Mo concentration. The aqueous-in-organic entrainment ratio for the model was set at 0.665 vol % for the 1A and 1B Banks and 1.75 vol % for the 1C, 1D, and 1E Banks, and the stage efficiency was set at 0.965, as discussed in Section 3.

As stated previously, the two principal objectives of the SASSE model are to determine if the 1EU product stream can meet the TVA specification for Mo content and to show that the solvent feed rates, in particular 1DX, are adequate to prevent refluxing of U and thereby ensure nuclear criticality safety. The question of U refluxing will be reviewed first, since refluxing criteria place limitations on the flow rates used in the SASSE model.

The H-Canyon DCA[4] places limits on the organic-to-aqueous volumetric flow ratios in First and Second Cycle to prevent the refluxing of U and thereby assure nuclear criticality safety. Notably, the (1AX + 1BS)/1CX flow ratio is restricted below certain levels, which decrease as the HNO_3 concentration in 1CU increases, and the 1DX/1DF flow ratio is restricted above certain levels, which increase as the U concentration in 1DF increases. The 1AX/1AF, 1AS/1AX, 1BX/1AX, and 1BS/1BX flow ratios also are restricted. The flow limits in the DCA are based on U distribution calculations for varying First and Second Cycle operating conditions.[4,31] The criterion used to determine U reflux was that the U concentration in either the organic or the aqueous phase in any stage must not exceed the U concentration in the feed solution.

The proposed flowsheet does not violate the DCA flow restrictions for 1A, 1B, and 1C Banks. Reflux of U in 1D Bank becomes a concern at the 1DF feed concentration of 20 g/L U. Figure 5-1 shows the H-Canyon DCA criticality limit for the 1DX/1DF volumetric flow ratio.[4,31] The applicable limiting flow ratio for 7.5 vol % TBP in 1DX and 1.0 M or less HNO_3 in 1DS is set by the 0.8 M HNO_3 line in Figure 5-1; permissible 1DX/1DF flow ratios are above and to the left of this line. From Table 3-1, the maximum flow 1DF flow rate for the proposed flowsheet is 8.13 L/min. To satisfy the DCA guidelines, the 1DF flow rate is multiplied by the minimum 1DX/1DF flow ratio at an estimated 1DF feed concentration of 25 g/L U, which from Figure 5-1 is approximately 4.05. The resulting minimum 1DX flow rate is 32.9 L/min.

To affirm that the SASSE model shows that there is no U reflux in 1D Bank, the onset of reflux was determined using the same criterion as for the DCA. The onset of reflux was calculated both for conditions that matched the original reflux analysis[19] and for the proposed flowsheet. The reflux criterion given by the left-hand curve in Figure 5-1 incorporates two changes from the proposed flowsheet (a lower TBP concentration in 1DX, 7.0 vol % versus 7.5 vol %, and a lower 1DS HNO_3 concentration, 0.8 M versus 0.9 M), both of which favor the onset of U reflux. Therefore, the left-hand curve in Figure 5-1 represents a conservative bounding criterion for the proposed flowsheet rather than an accurate indication of the onset of reflux. A more accurate indication can be obtained by comparing the SASSE model with the results of the original reflux analysis, shown by Figure 5-2.[19] The input to the SASSE spreadsheet was changed to be identical with that of the analysis for Figure 5-2, namely 4 M HNO_3 in 1DF, 1 M HNO_3 in 1DS, and a 1DS/1DX flow ratio of 0.15. The only difference between the SASSE calculations and the previous reflux analysis was the substitution of asymptotic expressions for HNO_3 and U(VI) distribution coefficient defined by equations 3 through 12 for the polynomial expressions used in the previous analysis, given by equations 1 and 2. At the higher U feed concentration of 20 g/L, SASSE calculations give a minimum 1DX/1DF flow ratio of 3.27 to prevent U reflux, compared to a minimum flow ratio of 2.7 from Figure 5-2. This comparison indicates that the SASSE model yields a slightly more restrictive 1D Bank reflux criterion than that defined by the DCA, or, in other words, that the SASSE model results conservatively bound the 1D Bank reflux criterion imposed by the DCA.

Another SASSE calculation was performed to compare the 1DX/1DF flow ratio at the adjusted 1DX flow rate of 33.5 L/min to the minimum flow ratio required to prevent U reflux. This calculation used the conditions for the proposed nominal flowsheet with 20 g/L U in 1DF. At these proposed flowsheet conditions, the minimum 1DX flow rate to prevent U reflux is

22.3 L/min. The 1DX/1DF flow ratio for the modified proposed flowsheet, 4.45, is more than 30% higher than the minimum flow ratio needed to prevent reflux, 3.02. Because the SASSE model has been shown to conservatively bound the limits of the DCA (from the comparison of SASSE calculations with Figure 5-2), one may conclude that 1D Bank will not reflux with 20 g/L in the 1DF feed, provided that the 1DX flow rate is set at 33.5 L/min.

A comparison of the Mo separation calculated by the SASSE model with the TVA specification for Mo impurities requires a conversion to account for blending of the product from 1EU with natural uranium. The TVA specification for Mo is <200 ppm by weight, or <200 μg Mo/g U, in the shipped product. Plans call for the enriched U (EU) product from the U/Mo separation to be blended at a 1:3.5 ratio with natural U (NU), which has a limit of <10 ppm by weight Mo, or <10 μg Mo/g U. Thus, the requirement for the 1EU product is (1+3.5) x 200 -3.5 x 10, or 865, μg Mo/g U. Allowances for uncertainties bring the practical limit down to about 800 μg Mo/g U for 1EU.

Table 5-1 and Figure 5-3 compare the U/Mo separations calculated by the SASSE model to the practical TVA limit of 800 μg Mo/g U. The results of the SASSE calculations indicate that the TVA limit should be met easily. The predicted levels of Mo in 1EU are less than 0.1 μg Mo/g U based on use of the Hallam data regression of the Mo distribution coefficient and 4 μg Mo/g U based on use of the Piqua data regression of the Mo distribution coefficient. The primary reason for the difference between the results for the Hallam-based and Piqua-based distribution coefficients is the lower value for the Hallam-based distribution coefficient, which causes the model to predict more efficient stripping of Mo into the aqueous phase in 1A Bank and, to a lesser extent, in 1D Bank.

It should be noted that the predicted success of the U/Mo separation is contingent on the ability of the 0.01 M HNO_3 to strip Mo in 1C and 1E Banks, if the SASSE model uses Mo distribution coefficients based on the Piqua data. The ability to strip Mo into the aqueous phase in dilute HNO_3 assumes that the Mo distribution coefficient continues to increase as the HNO_3 concentration drops from about 2-3 M (the lowest HNO_3 concentration for the Hallam and Piqua data, see Figures 9-14 and 9-15) to the dilute HNO_3 range.

Table 5-2 gives the predicted distribution of Mo, U, and Pu among all output streams from First and Second Cycle. As these tabulations indicate, the SASSE model predicts that nearly all of the U extracts into the organic phase in 1A, 1B, and 1D Banks and strips into the aqueous phase in 1C and 1E Banks. As a result, the SASSE model indicates that U losses should be low. (Actual U losses likely will be higher than the SASSE model shows, though still quite low.) The SASSE model predicts that Pu will quantitatively extract into the organic phase in 1A Bank as Pu(IV) and strip into 1BP in 1B Bank as Pu(III). If the Hallam or Piqua distribution coefficients are used, the model predicts that the Mo separation is less complete than for either U or Pu. Better separation is achieved with the lower values of the Mo distribution coefficient based on the regression of the Hallam data; this is not surprising, since the goal of the U/Mo separation is to simultaneously extract U into the organic phase and strip Mo into the aqueous phase. For the model using the Mo distribution coefficient based on the Piqua data, approximately 10% of the Mo remains in the product after 1A Bank; most of this is stripped out in 1C Bank. If the Mo distribution coefficient is based on the Visser and Pierce and the Fujii et al. data, the model

predicts that virtually all of the Mo will remain in the aqueous phase in 1A Bank and will be removed in the 1AW stream.

Figure 5-3 depicts predicted reductions in the Mo concentration in the output stream from each mixer-settler bank based on the Hallam and Piqua tests; predicted Mo concentrations based on the Visser and Pierce and Fujii et al. measurements are negligibly low and therefore are not shown. The results in Tables 5-1 and 5-2 and Figure 5-3 indicate that to be conservative the SASSE prediction of the Mo separation should be based on a Mo distribution coefficient from the correlation of the Piqua data. Use of a distribution coefficient based on either the Hallam or the Piqua data is conservative with respect to a distribution coefficient based on measured distribution data. The much lower measured distribution coefficients (see Figure 8-14) would result in virtually no extraction of Mo in 1A Bank and consequently a quantitative loss of virtually all Mo to 1AW.

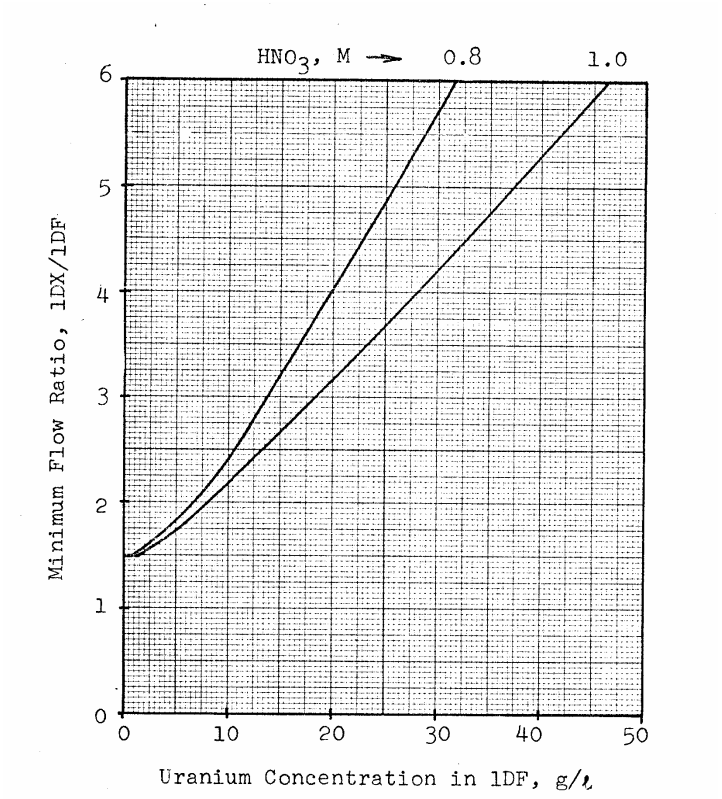

Figure 5-1. Limiting 1DX/1DF Flow Ratio in H-Canyon DCA

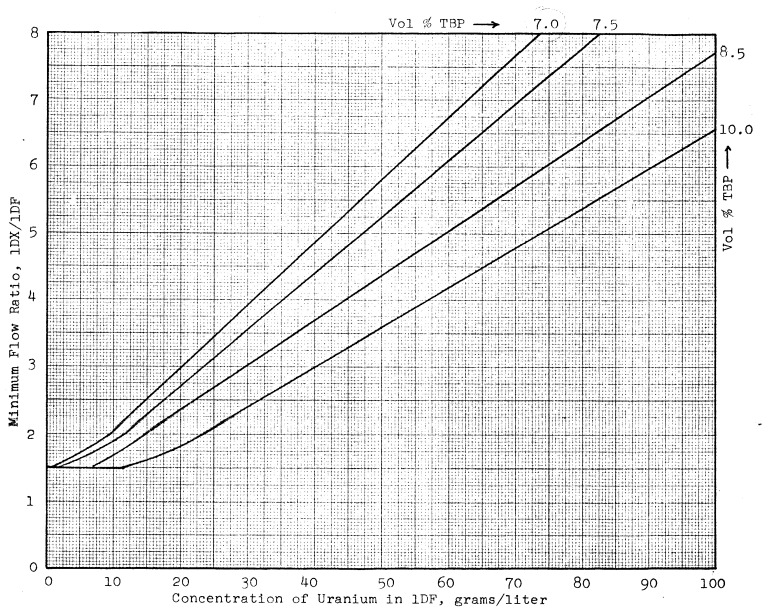

Figure 5-2. Calculated 1DX/1DF Flow Ratio at Onset of U Refluxing

Table 5-1. Molybdenum Levels in Product Streams for Proposed Flowsheet

Product Stream	**mg Mo/g U Hallam $D_{o/a}$**	**mg Mo/g U Piqua $D_{o/a}$**	**mg Mo/g U Visser $D_{o/a}$**
1AU	17	6764	3.7E-05
1BU	17	6690	7.1E-13
1CU	0.57	222	7.1E-13
1DU	0.15	172	6.9E-19
1EU	0.00	4.0	6.9E-19

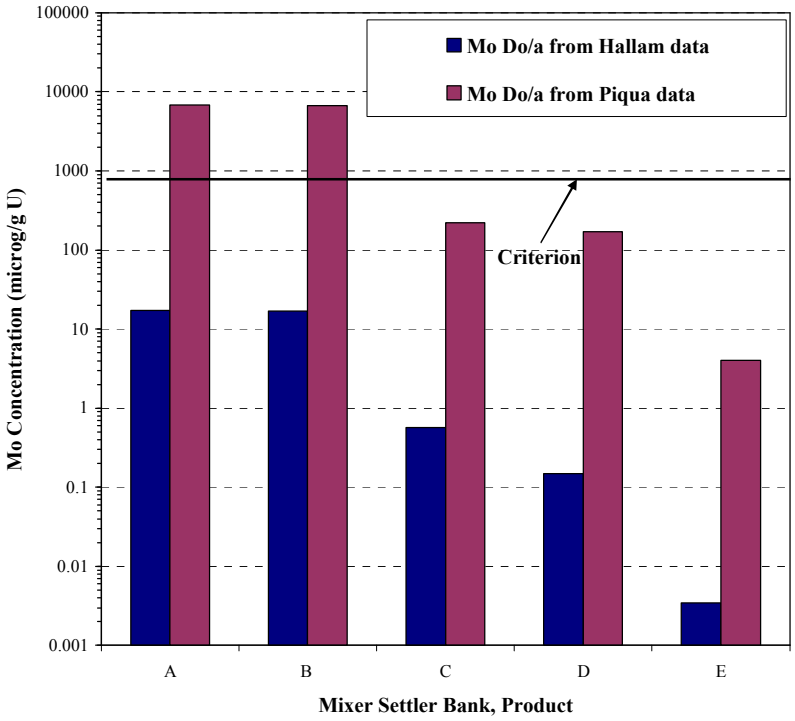

Figure 5-3. SASSE Predictions of Mo Contamination in First and Second Cycle Solvent Extraction Product Streams

Table 5-2. Percentage Distribution of Molybdenum, Uranium, and Plutonium among Proposed Flowsheet Output Streams

Molybdenum Distribution Coefficient for Hallam Fuel

	1AW	1BP	1CW	1DW	1EU	1EW
Mo	99.9845	<0.0001	0.0150	0.0004	<0.0001	0.0001
U	0.0001	0.0001	<0.0001	<0.0001	99.9998	<0.0001
Pu	<0.0001	>99.9999	<0.0001	<0.0001	<0.0001	<0.0001

Molybdenum Distribution Coefficient for Piqua Fuel

	1AW	1BP	1CW	1DW	1EU	1EW
Mo	93.9096	<0.0001	5.8888	0.0397	0.0038	0.1581
U	0.0001	0.0001	<0.0001	<0.0001	99.9998	0.0000
Pu	<0.0001	>99.9999	<0.0001	<0.0001	<0.0001	<0.0001

Molybdenum Distribution Coefficient for Visser and Pierce Tests

	1AW	1BP	1CW	1DW	1EU	1EW
Mo	>99.9999	<0.0001	<0.0001	<0.0001	<0.0001	<0.0001
U	0.0001	0.0001	<0.0001	<0.0001	99.9998	<0.0001
Pu	<0.0001	>99.9999	<0.0001	<0.0001	<0.0001	<0.0001

Figures 5-4 through 5-18 depict the stagewise equilibrium profiles for the SASSE model with the Mo distribution coefficient based on the Piqua data. The SASSE model confirms that U and Pu separate in 1B Bank, due to the FS addition in 1BX to reduce extractable Pu(IV) to inextractable Pu(III). The model shows that U and Mo separation occurs primarily in 1A Bank, where U extracts into the organic phase and most of the Mo remains in the aqueous phase, and 1C and 1E Banks, where U strips into the aqueous phase and Mo remains in the organic phase. The separation between U and Mo can be attributed to the increase in the extractability of molybdic acid as the HNO_3 concentration decreases, as noted Section 4. The amount of U/Mo separation in 1D Bank is less than in 1A Bank because of the higher organic/aqueous flow ratio in 1D Bank, which lowers the HNO_3 concentration and therefore increases the amount of Mo that extracts into the organic phase.

It is noteworthy that none of the profiles in Figures 5-4 through 5-18 exhibit any degree of refluxing. Refluxing would cause an intermediate peaking in concentration over one or more stages between the feed stage and the stages on either end of the mixer-settler banks.

A concern that the SASSE modeling does not address directly is the possibility of Mo precipitation. Solubility data for Mo in HNO_3 solutions containing from 0 to 360 g/L U at temperatures up to 100 °C[31] show that there is an envelope of peak Mo solubility that shifts to lower HNO_3 concentrations as the U concentration increases. The data also show that the Mo solubility decreases as the temperature increases. As part of the development of the proposed flowsheet, Mo solubilities were measured at conditions representative of the proposed fuel dissolver, namely, a temperature of 100 °C, a U concentration of 20 g/L, and initial HNO_3 concentrations of 4 to 6 M.[32] Results from these two sets of measurements are compared with the operating conditions for 1A Bank to demonstrate that Mo will not precipitate during the proposed solvent extraction process. At least 90% of the Mo strips into 1AW, as indicated by Table 5-2, so Mo solubility is a concern only in 1A Bank. The minimum measured Mo solubility of 0.72 g/L (in dilute HNO_3)[30] is sufficient to preclude the possibility of precipitation in any of the banks downstream from 1A Bank.

Figure 5-19 compares the conditions in 1A Bank with the low acid solubility limit for HNO_3 solutions with no U and the high acid solubility limit for HNO_3 solutions with 20 g/L U. Because the envelope of peak Mo solubility shifts to lower HNO_3 concentrations (to the left in Figure 5-19) as the U concentration increases, these two limiting curves combine to define a region of solubility for any solution containing between 0 and 20 g/L U. As Figure 5-19 shows, the operating conditions in 1A Bank lie entirely within this region of solubility; the closest approach to the solubility limit occurs in the stripping end of 1A Bank, where both the HNO_3 and Mo concentrations are highest. The solubility limits for Mo at the 1A Bank operating temperature of 40 °C are higher than shown in Figure 5-19, so the margin between the operating conditions and the solubility limits is larger than shown. It may be concluded that Mo will not precipitate in 1A Bank or anywhere in First or Second Cycle.

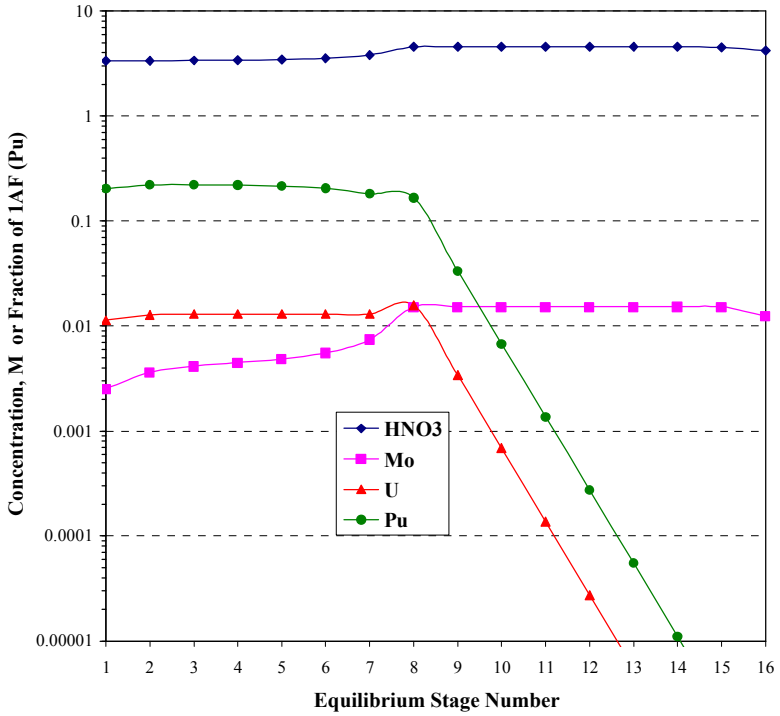

Figure 5-4. SASSE Predictions of Aqueous Phase Concentrations in 1A Bank for Proposed U/Mo Separation Flowsheet, with Mo $D_{o/a}$ Based on Piqua Tests

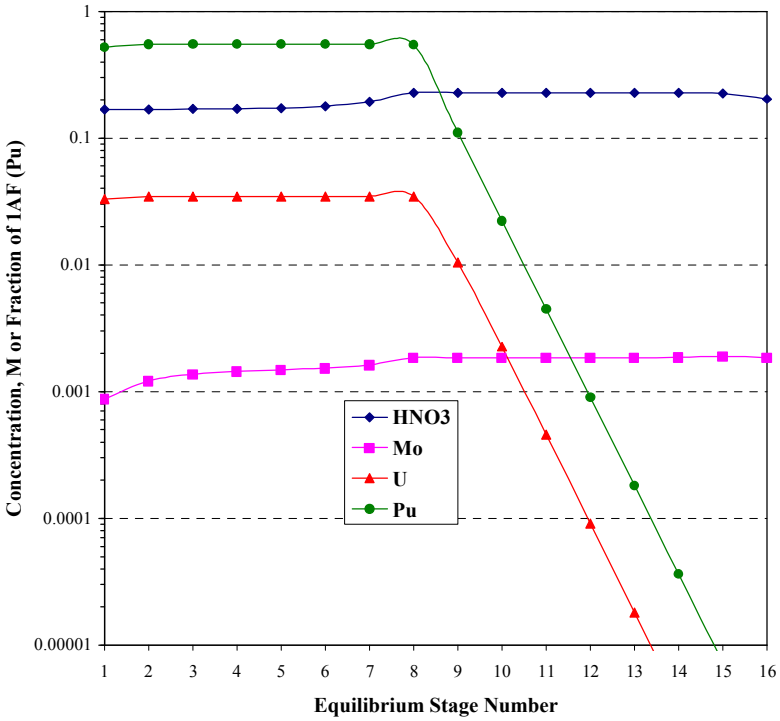

Figure 5-5. SASSE Predictions of Organic Phase Concentrations in 1A Bank for Proposed U/Mo Separation Flowsheet, with Mo $D_{o/a}$ Based on Piqua Tests

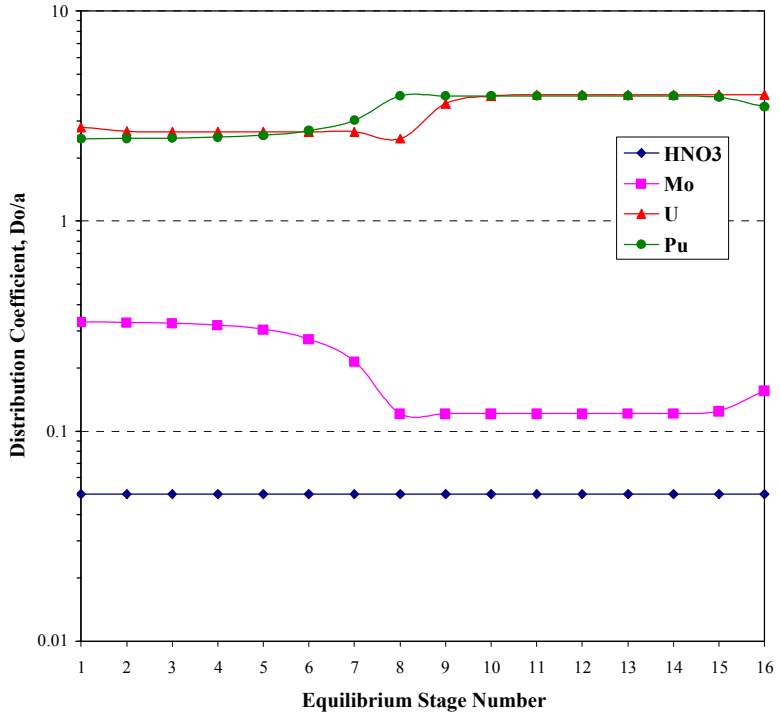

Figure 5-6. SASSE Predictions of Distribution Coefficients in 1A Bank for Proposed U/Mo Separation Flowsheet, with Mo $D_{o/a}$ Based on Piqua Tests

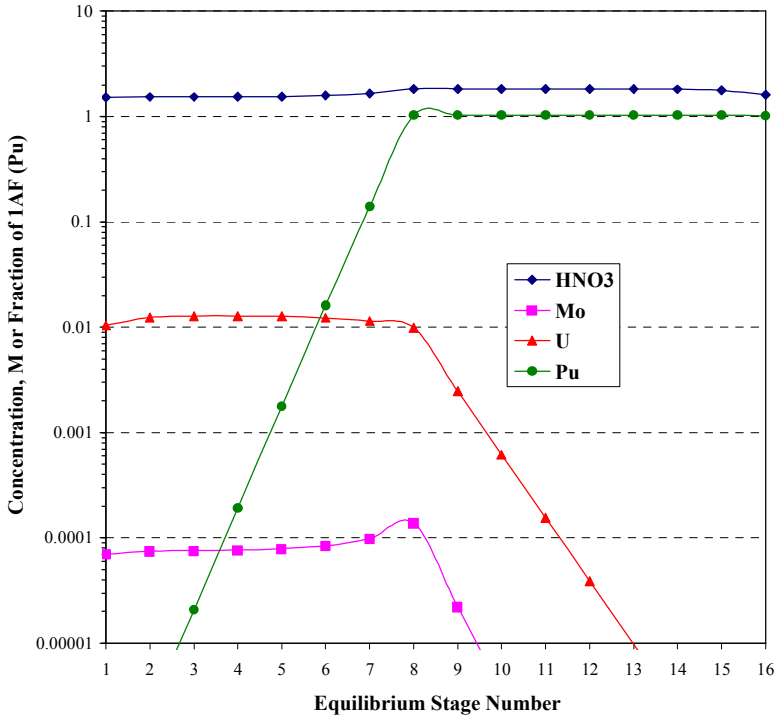

Figure 5-7. SASSE Predictions of Aqueous Phase Concentrations in 1B Bank for Proposed U/Mo Separation Flowsheet, with Mo $D_{o/a}$ Based on Piqua Tests

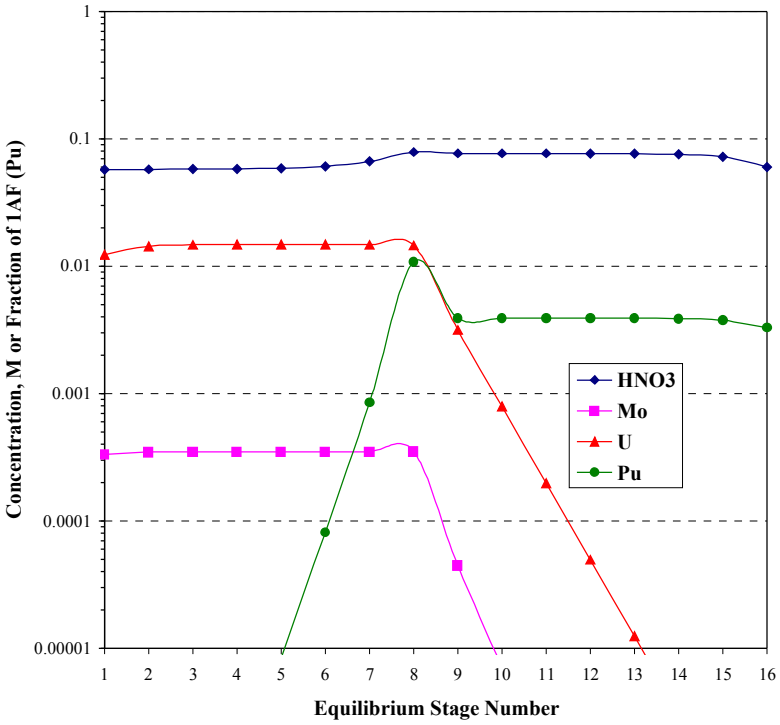

Figure 5-8. SASSE Predictions of Organic Phase Concentrations in 1B Bank for Proposed U/Mo Separation Flowsheet, with Mo $D_{o/a}$ Based on Piqua Tests

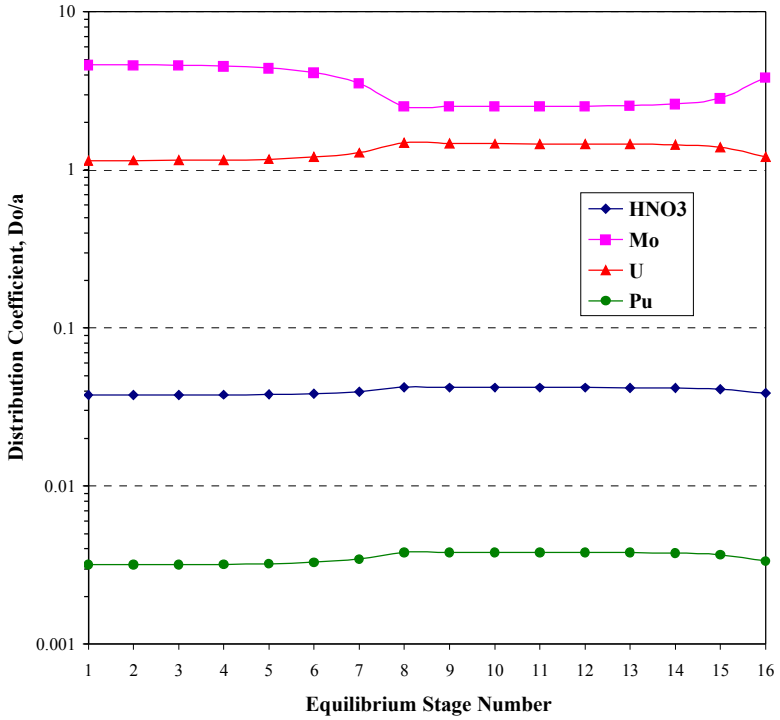

Figure 5-9. SASSE Predictions of Distribution Coefficients in 1B Bank for Proposed U/Mo Separation Flowsheet, with Mo $D_{o/a}$ Based on Piqua Tests

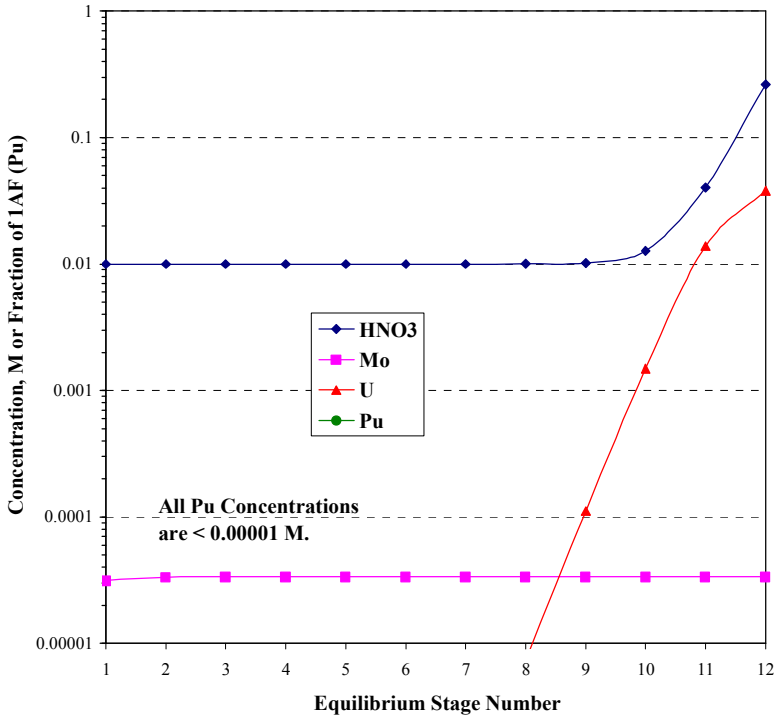

Figure 5-10. SASSE Predictions of Aqueous Phase Concentrations in 1C Bank for Proposed U/Mo Separation Flowsheet, with Mo $D_{o/a}$ Based on Piqua Tests

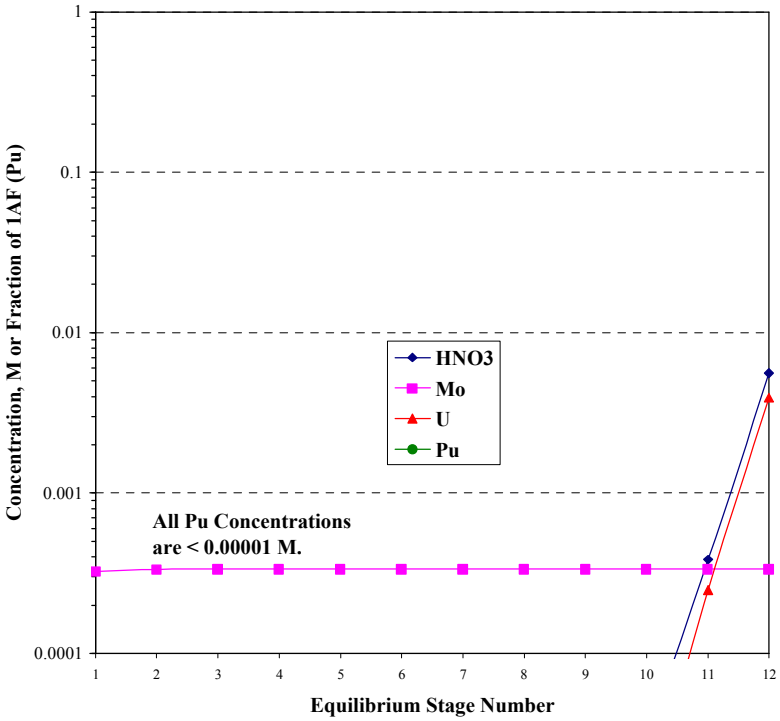

Figure 5-11. SASSE Predictions of Organic Phase Concentrations in 1C Bank for Proposed U/Mo Separation Flowsheet, with Mo $D_{o/a}$ Based on Piqua Tests

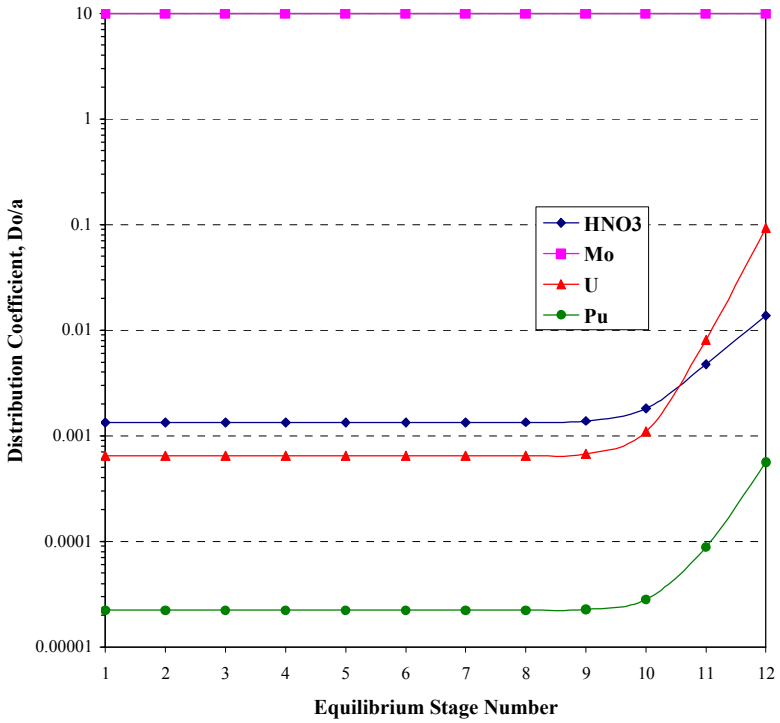

Figure 5-12. SASSE Predictions of Distribution Coefficients in 1C Bank for Proposed U/Mo Separation Flowsheet, with Mo $D_{o/a}$ Based on Piqua Tests

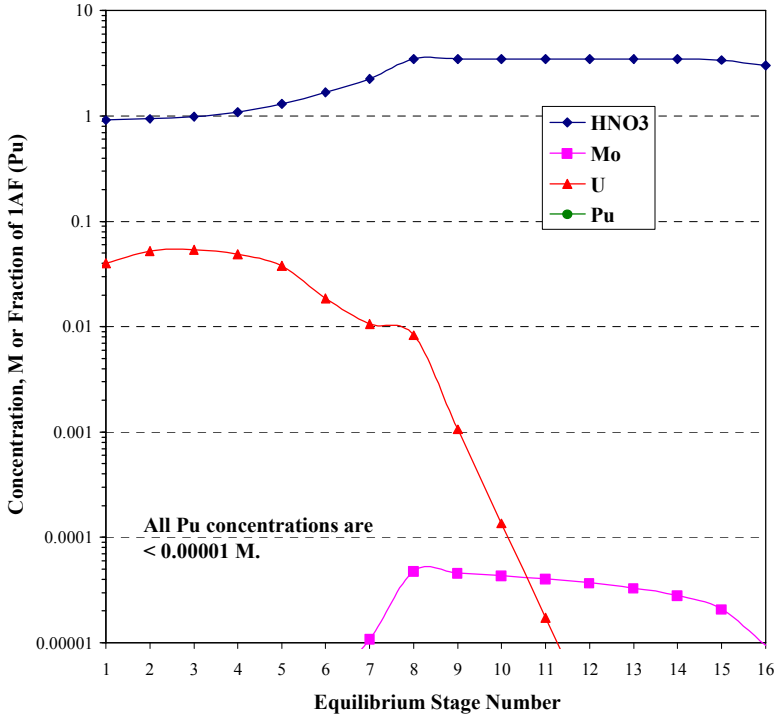

Figure 5-13. SASSE Predictions of Aqueous Phase Concentrations in 1D Bank for Proposed U/Mo Separation Flowsheet, with Mo $D_{o/a}$ from Piqua Tests

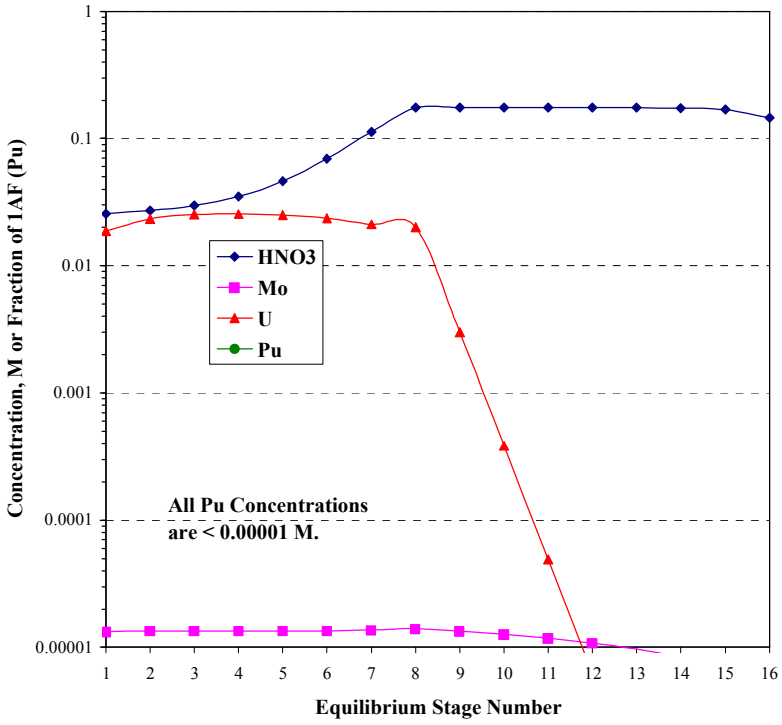

Figure 5-14. SASSE Predictions of Organic Phase Concentrations in 1D Bank for Proposed U/Mo Separation Flowsheet, with Mo $D_{o/a}$ from Piqua Tests

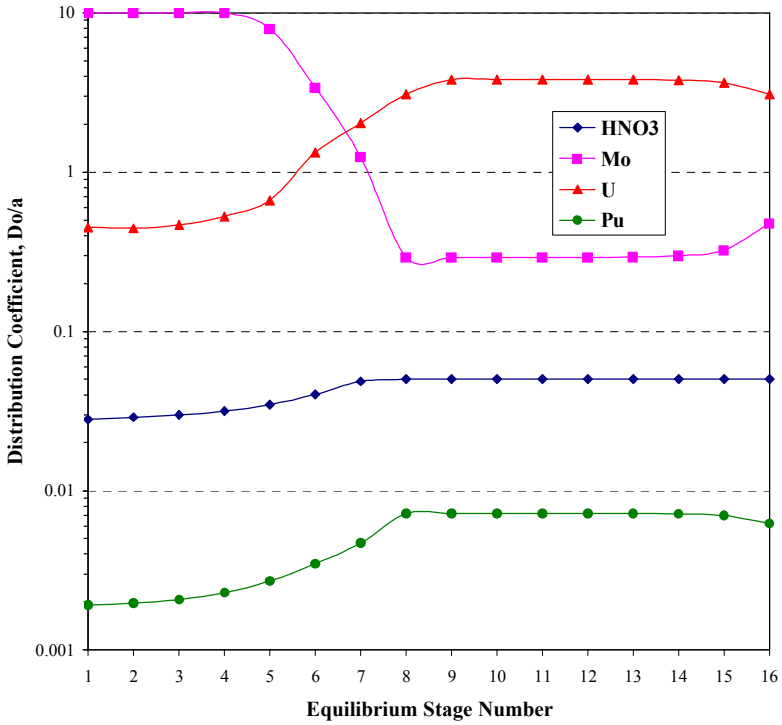

Figure 5-15. SASSE Predictions of Distribution Coefficients in 1D Bank for Proposed U/Mo Separation Flowsheet, with Mo $D_{o/a}$ from Piqua Tests

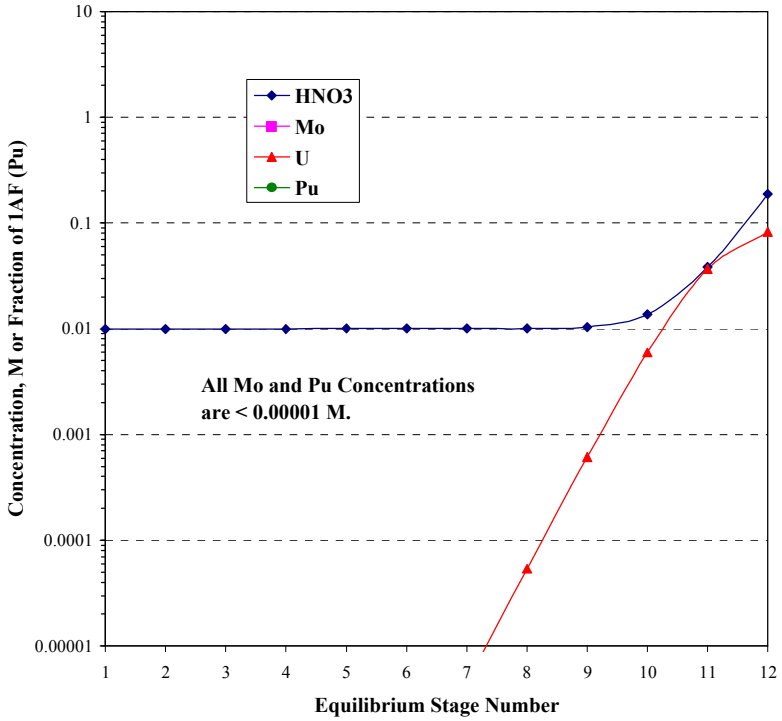

Figure 5-16. SASSE Predictions of Aqueous Phase Concentrations in 1E Bank for Proposed U/Mo Separation Flowsheet, with Mo $D_{o/a}$ from Piqua Tests

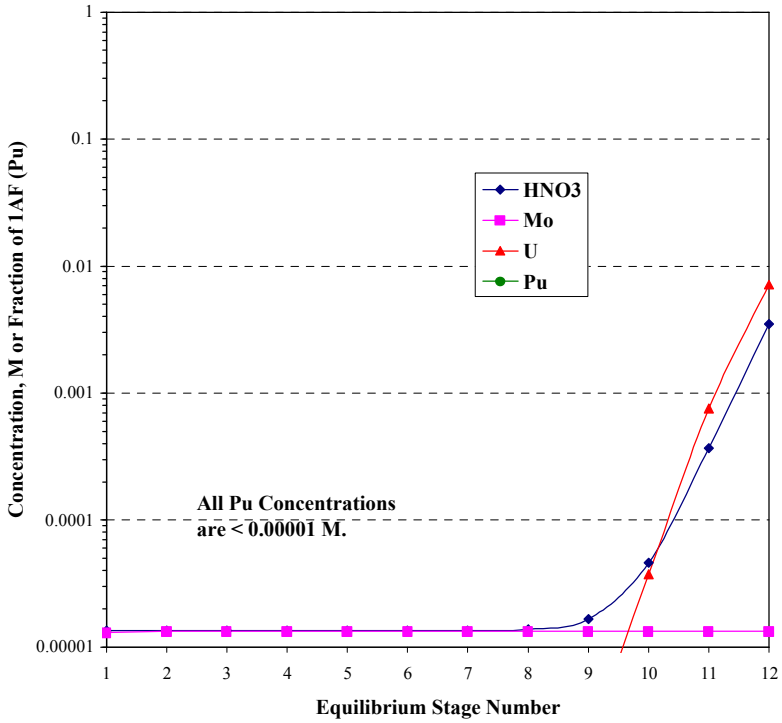

Figure 5-17. SASSE Predictions of Organic Phase Concentrations in 1E Bank for Proposed U/Mo Separation Flowsheet, with Mo $D_{o/a}$ from Piqua Tests

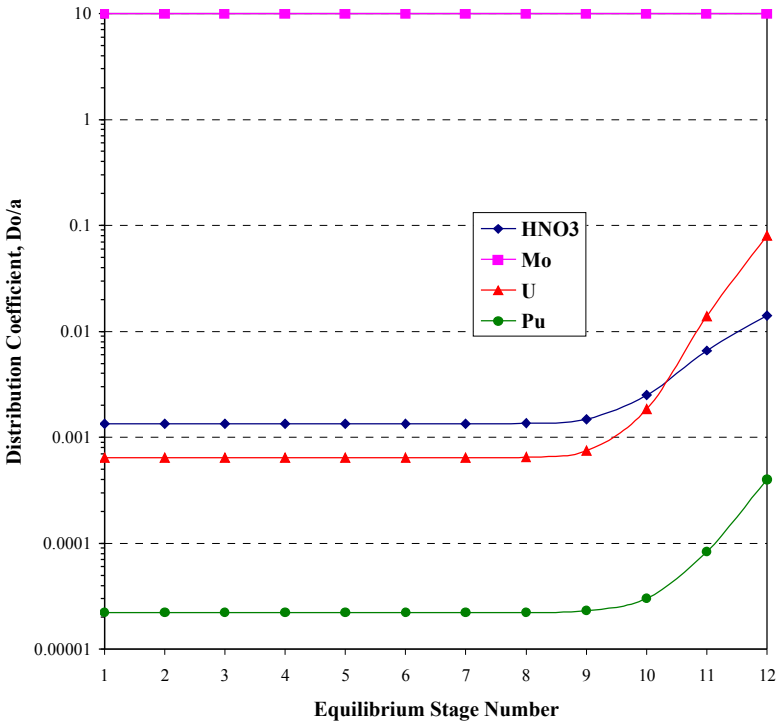

Figure 5-18. SASSE Predictions of Distribution Coefficients in 1E Bank for Proposed U/Mo Separation Flowsheet, with Mo $D_{o/a}$ from Piqua Tests

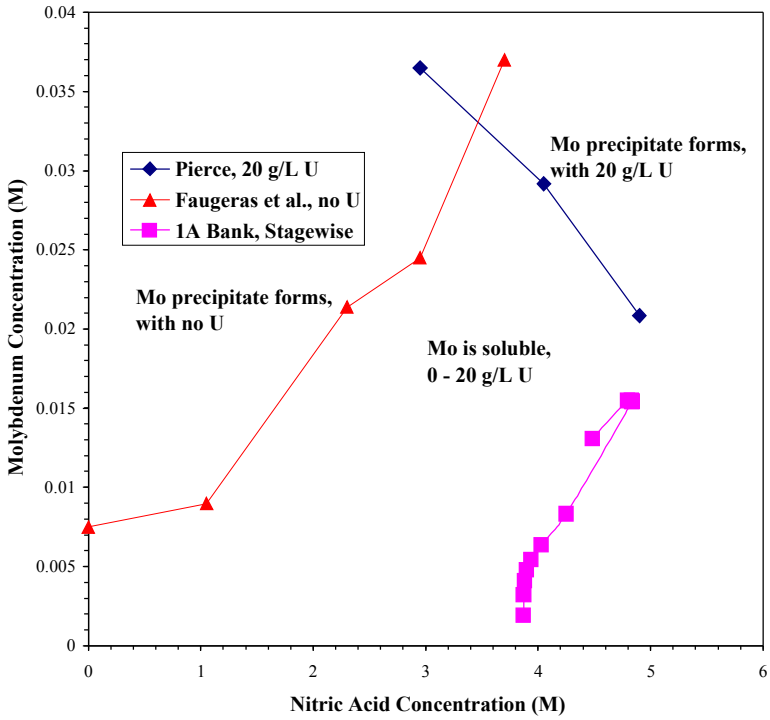

Figure 5-19. Comparison of 1A Bank Operating Conditions with Molybdenum Solubility Limits at 100 °C

6.0 CONCLUSIONS

SASSE spreadsheet models of H-Canyon First and Second Cycle solvent extraction show that a standard unirradiated fuel flowsheet is capable of separating U from Mo in dissolved solutions of a U/Mo alloy. The standard unirradiated fuel flowsheet is used, except for increases in solvent feed rates to prevent U refluxing and thereby ensure nuclear criticality safety and substitution of higher HNO_3 concentrations for aluminum nitrate ($Al(NO_3)_3$) in the feed to 1A Bank.

The TVA limit for the final blended product is 200 μg Mo/g U, which translates to approximately 800 μg Mo/g U for the Second Cycle product solution. Conservative SASSE calculations, based on Mo organic-to aqueous distributions measured during minibank testing for previous processing of Piqua reactor fuel, give a Mo impurity level of 4 μg Mo/g U in the Second Cycle product solution. The calculated impurity level is slightly more than two orders of magnitude lower than the required level. SASSE calculations based on measured Mo distributions, from Visser and Pierce and Fujii et al. tests, indicate that there virtually all of the Mo will be removed in 1A Bank and that, consequently, there will be no Mo impurities in the Second Cycle product solution.

The 1DF U concentration of 20 g/L specified by the proposed flowsheet requires an increased 1DX organic feed rate to satisfy H-Canyon DCA guidelines for the prevention of U refluxing.[4] First cycle flows also require adjustment to account for the increased U concentration in 1AF. The ranges for the 1AX, 1BS, and 1DX organic flow rates in the proposed flowsheet are set so that the limiting ratios of organic/aqueous flow rates exactly meet the minimum values specified by the DCA.[4]

7.0 REFERENCES

[1] R. A. Pierce, "Flowsheet Evaluation for the Processing of U-Mo Materials in H-Canyon," WSRC-STI-2006-00363, Rev. 0, December, 2006.
[2] DE-SA09-01SR18976, "Interagency Agreement Between DOE and TVA For The Off-Specification Fuel Project," April 5, 2001.
[3] R. A. Leonard and M. C. Regalbuto, "A Spreadsheet Algorithm for Stagewise Solvent Extraction," Sol. Extr. And Ion Exch., 12(5), 909-930, 1994.
[4] L. M. Gundy, "H-Canyon Double Contingency Analysis," N-NCS-H-00037, Rev. 15, March, 2006.
[5] A. D. Mitchell, "SEPHIS-MOD4: A User's Manual to a Revised Model of the Purex Solvent Extraction System," Oak Ridge National Laboratory Report ORNL-5471, May, 1979.
[6] J. E. Laurinat, "SASSE Modeling of First Cycle Neptunium (VI) Recovery Flowsheet," WSRC-TR-2006-00104, Rev. 0, April, 2006.
[7] J. E. Laurinat, "SASSE Modeling of First Cycle Neptunium (IV) Flowsheet," WSRC-TR-2006-00187, Rev. 0, June, 2006.
[8] M. C. Thompson, "Solvent Extraction of Off-Site Fuels Containing Mo and Zr," DPST-73-469, October 15, 1973.
[9] E. G. Orebaugh, "RTA 907-S, Hallam Fuel (U-10-Mo) Flowsheet Studies," DPST-79-464, July 13, 1979.
[10] S. L. Hudlow, "First Cycle Operating Ranges and PPL's for Unirradiated Mk 22 Assemblies and Unblended INEEL Materials," X-CLC-H-00074, Rev. 16, April 24, 2006.
[11] E. A. Kyser, "Validation of the SEPHIS Program for the Modeling of the HM Process," WSRC-TR-98-00376, Rev. 0, October, 1998.
[12] M. L. Hyder, W. C. Perkins, M. C. Thompson, G. A. Burney, E. R. Russell, H. P. Holcomb, and L. F. Landon, "Processing of Irradiated Enriched Uranium Fuels at the Savannah River Plant," DP-1500, April, 1979.
[13] J. W. Ward, "Reduction of Entrainment of Purex 1AS into 1AP," DPSOX 7667, September 17, 1970.
[14] J. B. Starks, "Determination of Entrainment of Purex 1AS into 1AP," DPSOX 7942, November 24, 1971.
[15] C. E. Pickett, "Questions Concerning 1CU Conductivity Meter Alarm Limit Calculations," NMS-EHA-2000-00040, March 2, 2000.
[16] C. E. Pickett, "Capacity of Second Neptunium Cycle vs. Entrainment," 221H-LIB-F-26-006, December 8, 1969.
[17] M. L. Crowder, personal communication.
[18] T. H. Siddall III, S. G. Parker, and W. E. Prout, "Equilibrium Distribution Data for Purex and Similar Extraction Processes," DP-53, July, 1957.
[19] M. C. Thompson, B. E. Murphree, and R. L. Shankle, "Equilibrium Distribution of Uranyl Nitrate between Nitric Acid and 7.5 vol % TBP," DP-1384, October, 1975.
[20] M. C. Thompson, "Second Cycle Solvent Extraction Purification of Uranium," DPST-72-478, October 23, 1972.
[21] L. L. Smith, "Solvent Extraction Data for Plutonium: A Compilation of Data in the Literature," DP-700, December, 1962, Tables I and II.

[22] G. F. Best, H. A. C. McKay, and P. R. Woodgate, "Tri-n-Butyl Phosphate as an Extracting Solvent for Inorganic Nitrates – III, The Plutonium Nitrates," J. Inorg. Nucl. Chem., 4, 315-320, 1957.
[23] G. Carleson, "The Extraction of Plutonium at Various Oxidation Potentials," Proc. U. N. Intern. Conf. Peaceful Uses Atomic Energy, 2nd, Geneva, 17, P/137, 111-117, 1958.
[24] J. W. Codding, W. O. Haas, Jr., and F. K Heumann, "Tributyl Phosphate – Hydrocarbon Systems," Ind. Eng. Chem., 50, 145-152, 1958.
[25] N. R. Geary, "Collected Partition Data for Tri-Butyl Phosphate," United Kingdom Atomic Energy Authority, Windscale Works, Research and Development Report RDB(W)-8242, 1959.
[26] S. P. Vorob'ev, I. P. Davydov, and I. V. Shilin, "Polymerisation of Mo^{VI} in Acid Solutions," Russ. J. Inorg. Chem. (Engl. Transl.), 12(10), 1406-1411, 1967.
[27] T. Fujii, H. Yamana, M. Watanabe, and H. Moriyama, "Extraction of Molybdenum from Nitric Acid by Octyl(Phenyl) –*N,N*-Diisobutylcarbamoylmethylphosphine Oxide," Solvent Extr. Ion Exch., 19(1), 127-141, 2001.
[28] A. E. Visser and R. A. Pierce, "Solvent Extreaction for Uranium-Molybdenum Alloy Dissolution Flowsheet, WSRC-STI-2007-00129, Rev. 0, May, 2007.
[29] L. M. Ferris, "Aqueous Processes for Dissolution of Uranium-Molybdenum Alloy Reactor Fuel Elements," Oak Ridge National Laboratory Report ORNL-3068, July 14, 1961.
[30] P. Faugeras, C. Lehereux, and P. Leroy, "Étude de Solubilité du Molybdène en Milieu Nitrique," Commisseriat à l'Énergie Atomique (CEA) Report 1823, 1961.
[31] M. C. Thompson, "Solvent Extraction of Enriched Uranium in 221-H Using 7.5% TBP," DPST-73-477, October 29, 1973.
[32] R. A. Pierce, "Uranium-Molybdenum Dissolution Flowsheet Studies," WSRC-STI-2007-00103, Rev. 0, March, 2007.

8.0 APPENDIX: CORRELATION OF DISTRIBUTION COEFFICIENTS

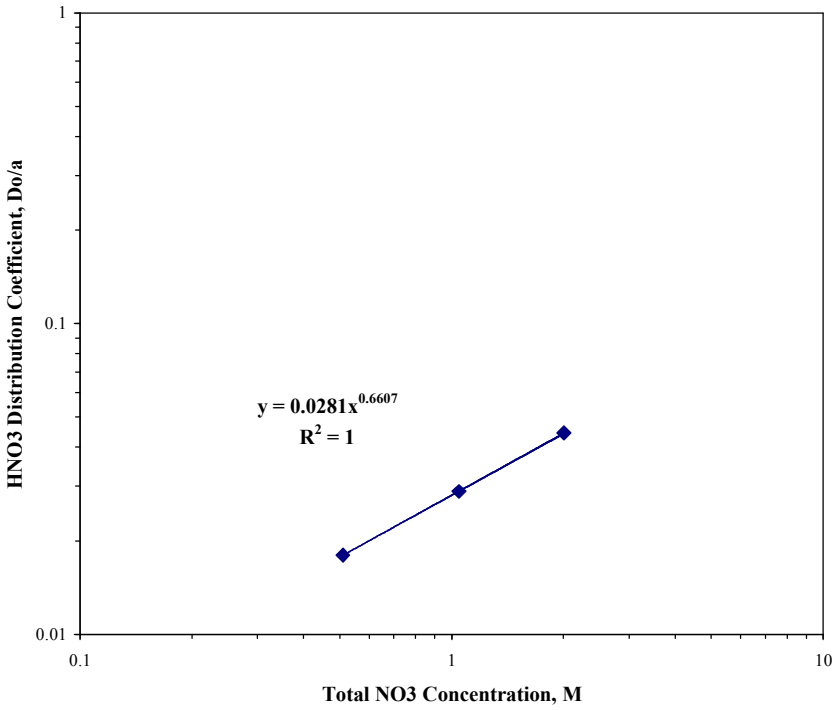

Figure 8-1. Correlation of HNO_3 Distribution Coefficient at Low U(VI) Concentrations

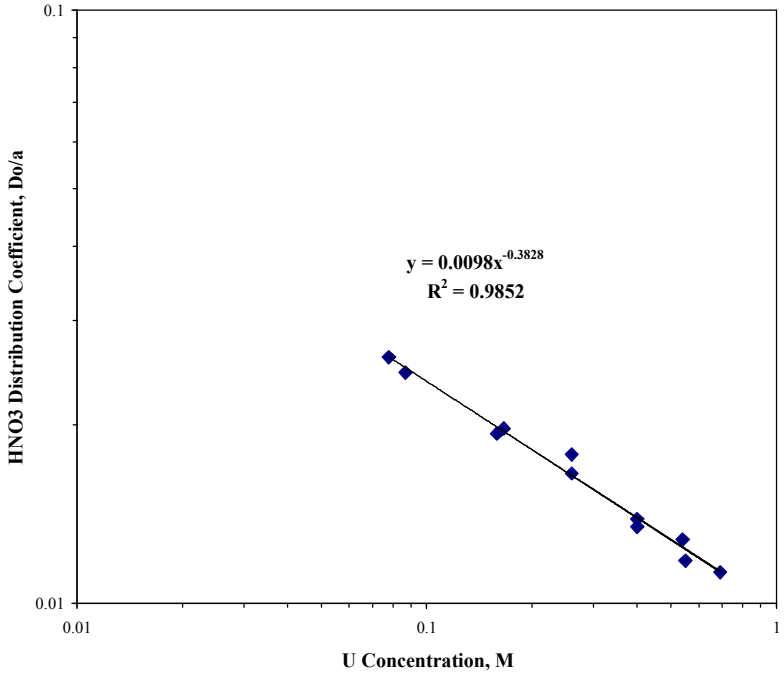

Figure 8-2. Correlation of Upper Asymptote to HNO_3 Distribution Coefficient, at Higher HNO_3 Concentrations

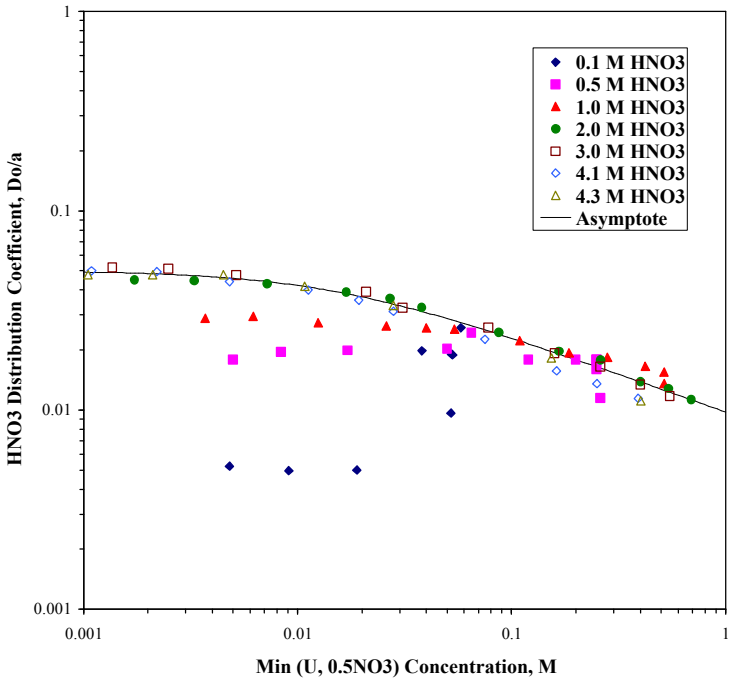

Figure 8-3. Correlation of Upper Asymptote to HNO_3 Distribution Coefficient

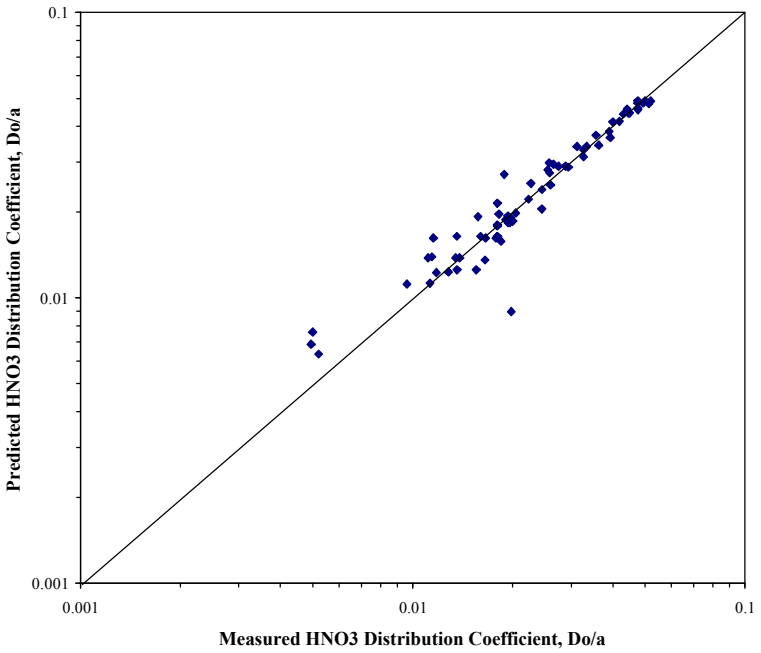

Figure 8-4. Predicted vs. Measured HNO_3 Distribution Coefficients

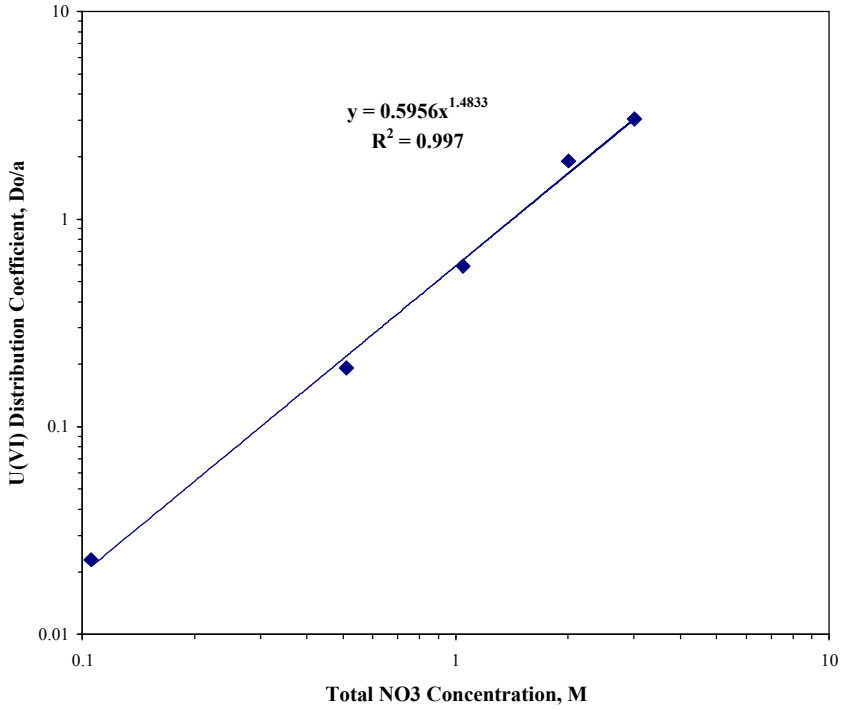

Figure 8-5. Correlation of U(VI) Distribution Coefficient at Low U(VI) and HNO_3 Concentrations

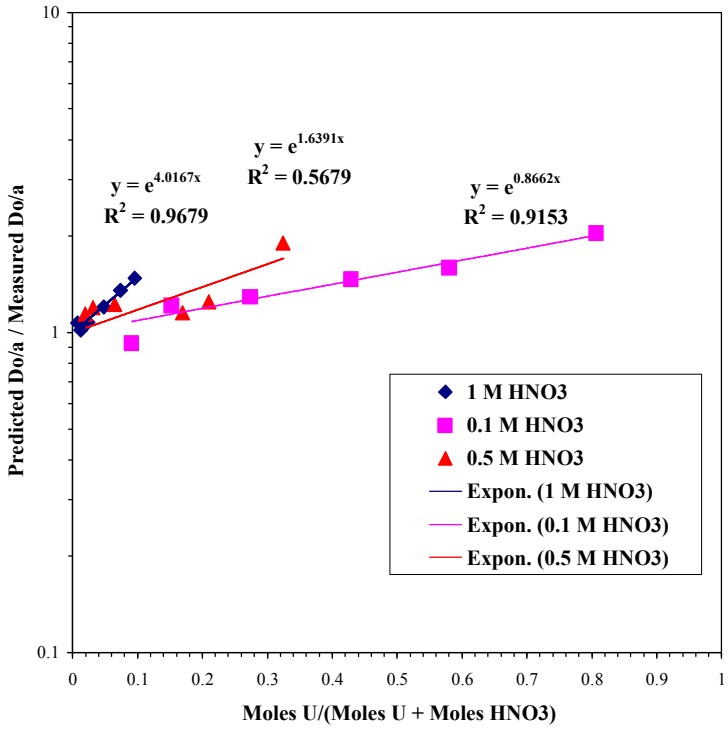

Figure 8-6. Correlation of U(VI) Salting Effect on U(VI) Distribution Coefficient

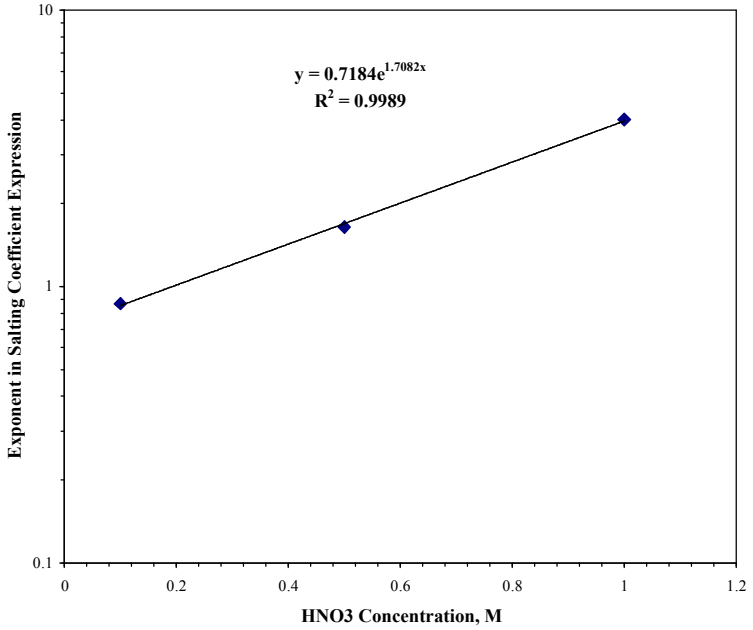

Figure 8-7. Correlation of Salting Factor for U(VI) Distribution Coefficient

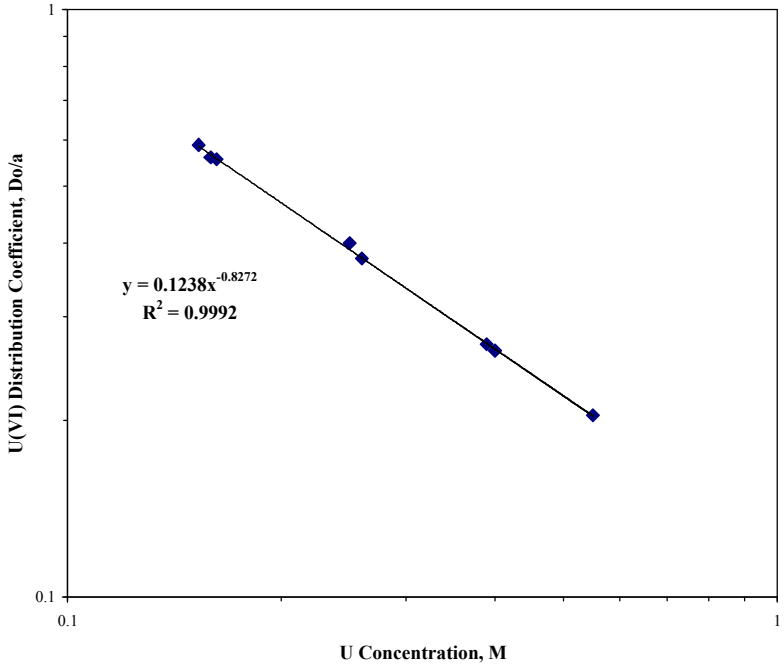

Figure 8-8. Correlation of Upper Asymptote to U(VI) Distribution Coefficient, at Higher U(VI) Concentrations

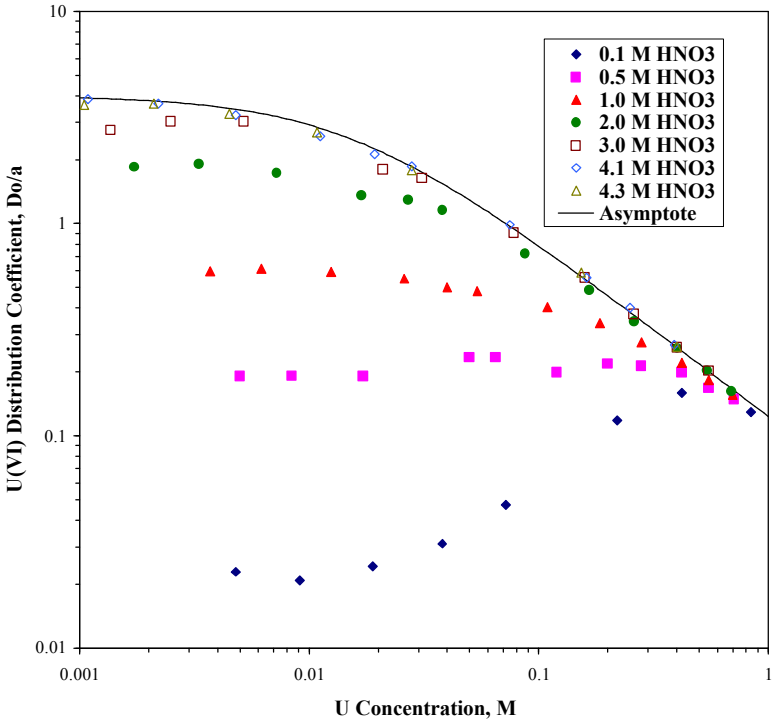

Figure 8-9. Correlation of Upper Asymptote to U(VI) Distribution Coefficient

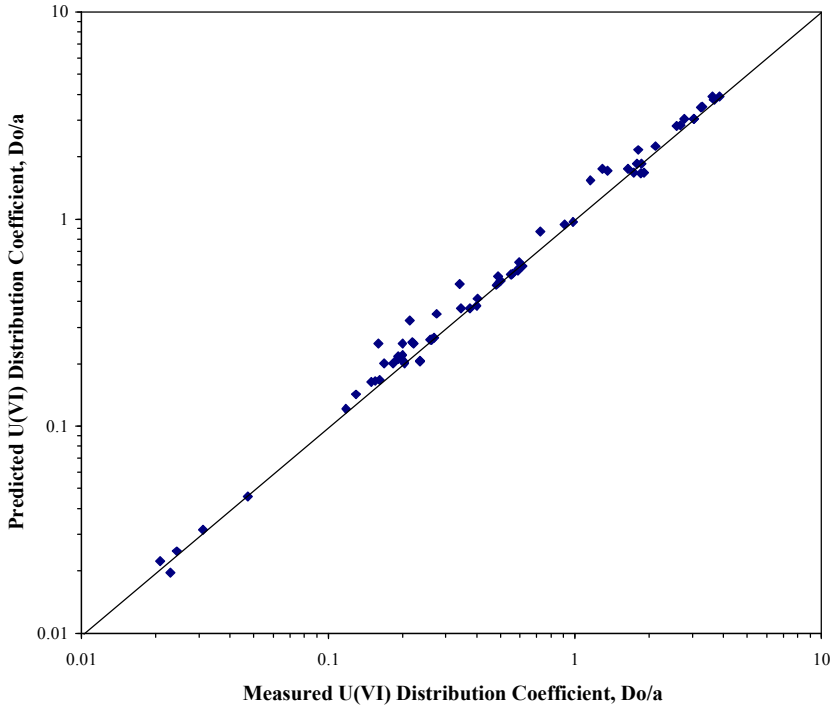

Figure 8-10. Predicted vs. Measured U(VI) Distribution Coefficients

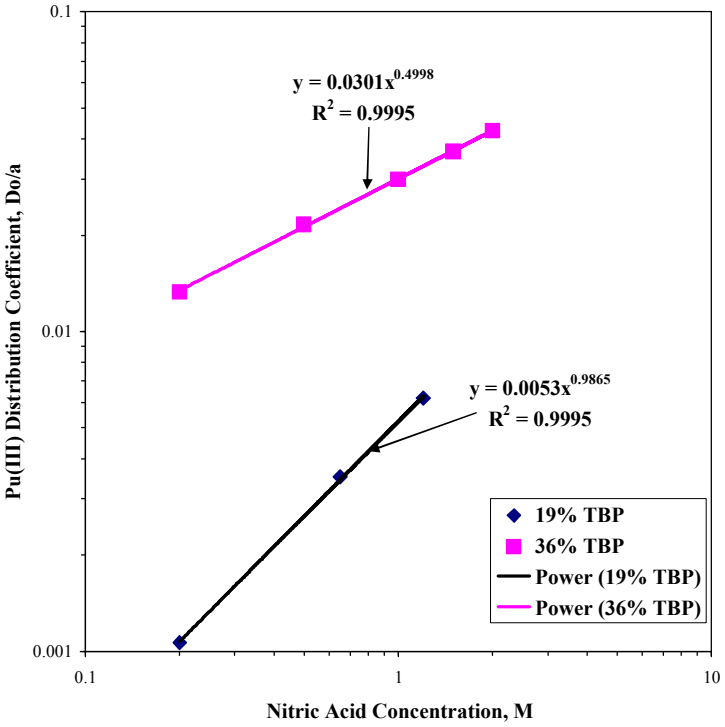

Figure 8-11. Correlation of Distribution Coefficient for Plutonium(III)

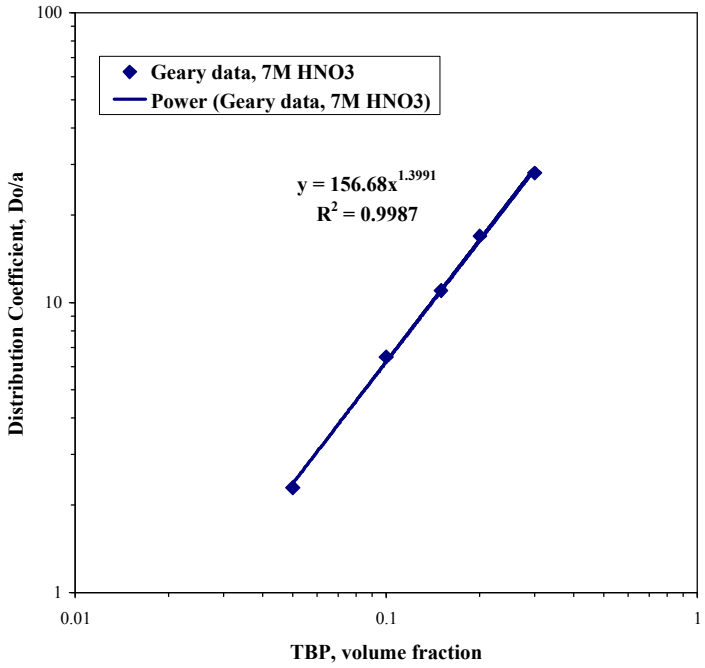

Figure 8-12. Correlation of Effect of TBP Concentration on Do/a for Pu(IV)

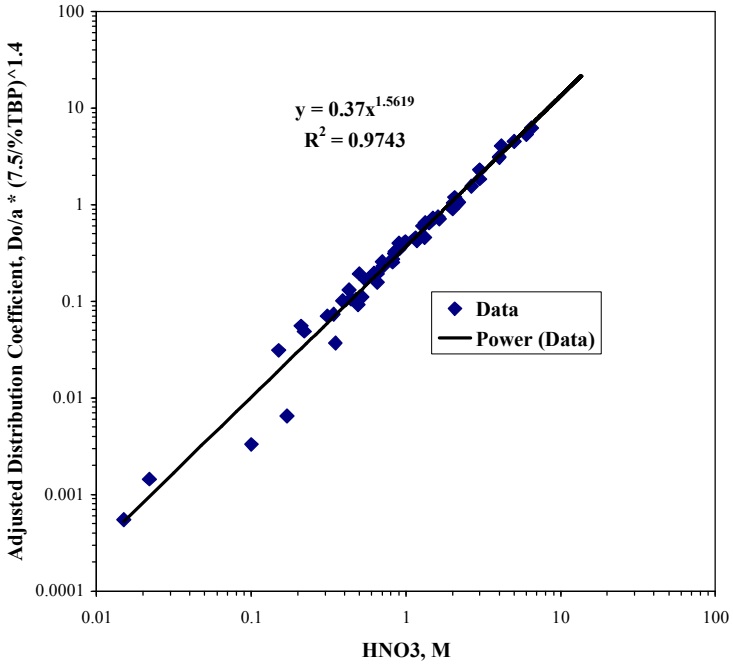

Figure 8-13. Correlation of Distribution Coefficient for Pu(IV) in 7.5 vol % TBP

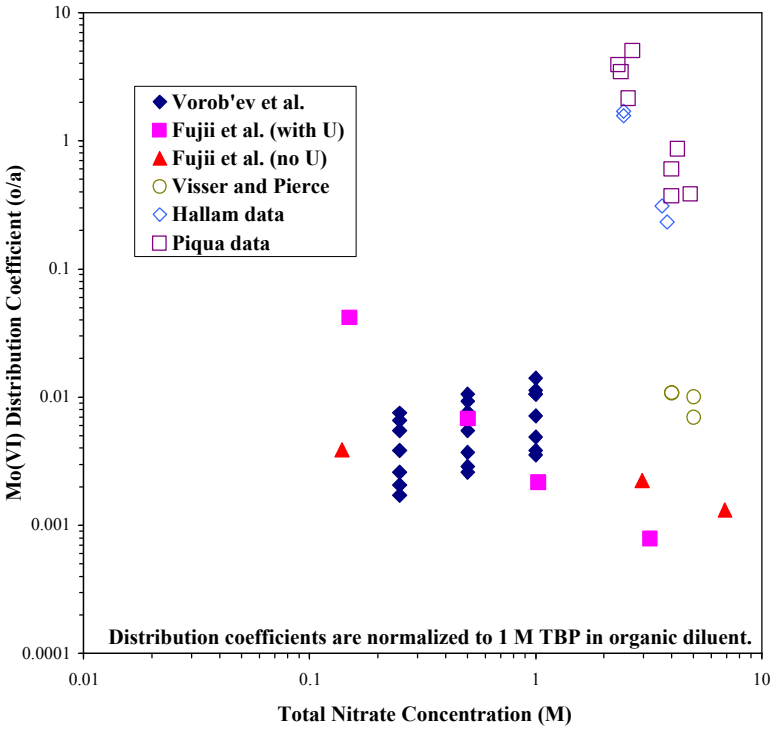

Figure 8-14. Comparison of Fitted Mo(VI) Distribution Coefficients for Hallam and Piqua Tests with Measured Distributions

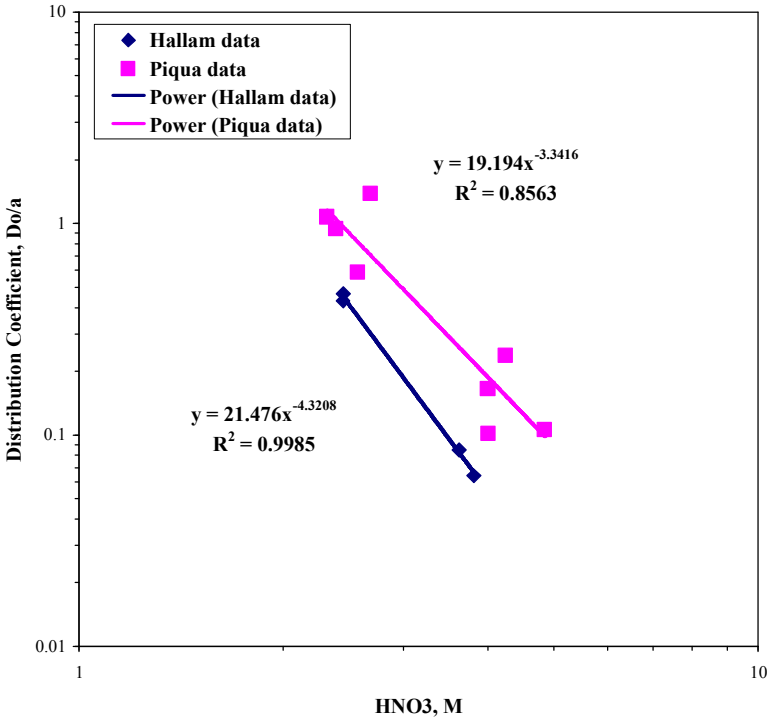

Figure 8-15. Correlations of Distribution Coefficients for Hallam and Piqua Tests

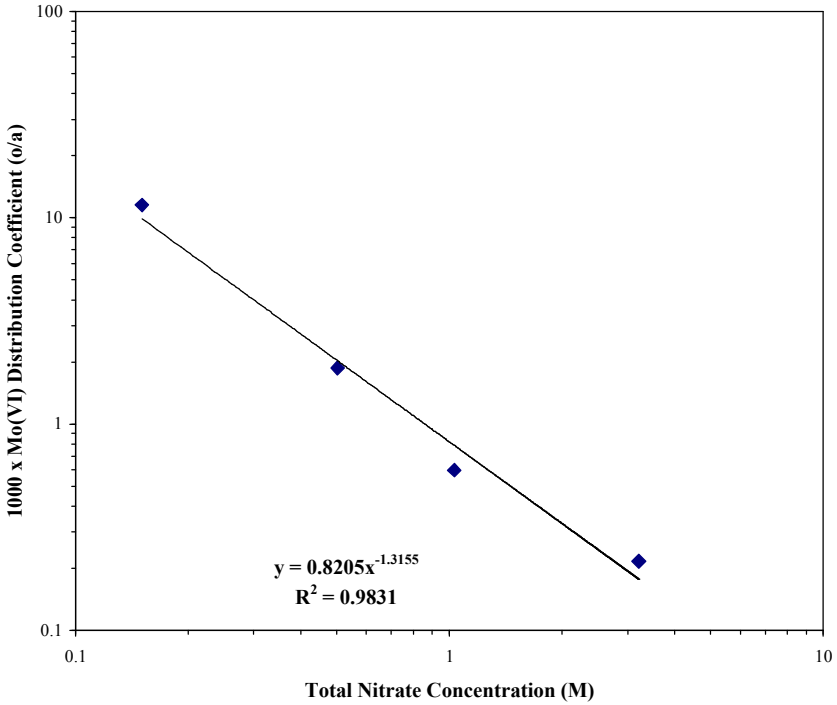

Figure 8-16. Correlation of Fujii et al. Mo(VI) Distribution Coefficients with U Present